AD-A169 731 PARAMETERIZATION OF OVERWATER DIFFUSION: SEPARATION OF RELATIVE DIFFUSION..(U) NAVAL POSTGRADUATE SCHOOL MONTEREY CA C E SKUPNIEWICZ ET AL. FEB 86 1/1

UNCLASSIFIED NEPRF-CR-86-02 N66856-85-WR-5019 F/G 4/1 NL

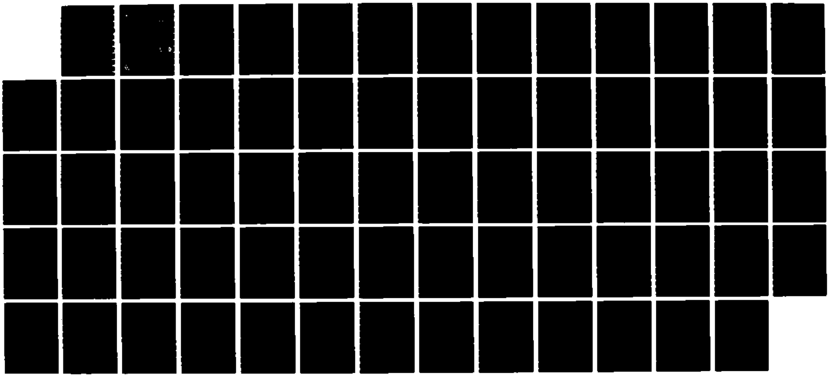

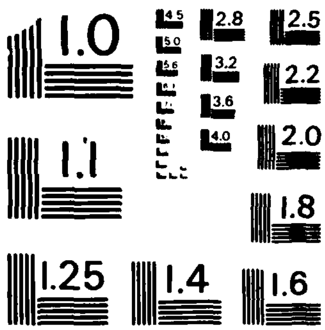

MICROCOPY RESOLUTION TEST CHART
NATIONAL BUREAU OF STANDARDS-1963-A

(12)

NAVENVPREDRSCHFAC
CONTRACTOR REPORT
CR 86-02

PARAMETERIZATION OF OVERWATER DIFFUSION: SEPARATION OF RELATIVE DIFFUSION AND MEANDER

C.E.Skupniewicz, G.E. Schacher, G.T. Vaucher

Naval Postgraduate School
Monterey, CA 93943

Contract No. N6685685WR85019

FEBRUARY 1986

Prepared For:
NAVAL ENVIRONMENTAL PREDICTION RESEARCH FACILITY
MONTEREY, CALIFORNIA 93943-5006

UNCLASSIFIED

SECURITY CLASSIFICATION OF THIS PAGE

REPORT DOCUMENTATION PAGE

1a REPORT SECURITY CLASSIFICATION UNCLASSIFIED	1b RESTRICTIVE MARKINGS
2a SECURITY CLASSIFICATION AUTHORITY	3 DISTRIBUTION / AVAILABILITY OF REPORT Approved for public release; distribution is unlimited
2b DECLASSIFICATION / DOWNGRADING SCHEDULE	
4 PERFORMING ORGANIZATION REPORT NUMBER(S)	5 MONITORING ORGANIZATION REPORT NUMBER(S) CR 86-02
6a NAME OF PERFORMING ORGANIZATION Naval Postgraduate School	6b OFFICE SYMBOL (If applicable) Code 61
7a NAME OF MONITORING ORGANIZATION Naval Environmental Prediction Research Facility	
6c ADDRESS (City, State, and ZIP Code) Monterey, CA 93943-5000	7b ADDRESS (City, State, and ZIP Code) Monterey, CA 93943-5006
8a NAME OF FUNDING / SPONSORING ORGANIZATION Naval Air Systems Command	8b OFFICE SYMBOL (If applicable) Air-330
9 PROCUREMENT INSTRUMENT IDENTIFICATION NUMBER N6685685WR85019	
8c ADDRESS (City, State, and ZIP Code) Department of the Navy Washington, DC 20361	10 SOURCE OF FUNDING NUMBERS

PROGRAM ELEMENT NO	PROJECT NO	TASK NO	WORK UNIT ACCESSION NO
62759N	WF59-551		DN654794

11 TITLE (Include Security Classification)
Parameterization of Overwater Diffusion: Separation of Relative Diffusion and Meander (U)

12 PERSONAL AUTHOR(S)
Skupniewicz, C.E.; Schacher, G.E.; Vaucher, G.T.

13a TYPE OF REPORT	13b TIME COVERED	14 DATE OF REPORT (Year, Month, Day)	15 PAGE COUNT
Final	FROM 3/1/85 TO 12/31/85	1986, February	65

16 SUPPLEMENTARY NOTATION

17 COSATI CODES

FIELD	GROUP	SUB-GROUP
04	01	
04	02	

18 SUBJECT TERMS (Continue on reverse if necessary and identify by block number)
Diffusion; Turbulence; Meander; Atmospheric modeling; Planetary boundary layer

19 ABSTRACT (Continue on reverse if necessary and identify by block number)

Data compiled from surface releases of SF6 gas in a purely over-water environment are used to parameterize both relative and single-particle diffusion in the lateral direction. Relative diffusion is found to be adequately described by surface layer stability for ranges to 10 km. Single-particle diffusion, often referred to as meander, is not found to be strongly related to surface layer stability, but does correlate well with measured lateral wind direction variance. A ~~Taylor's~~ (1921) "near field" approximation closely predicts the single-particle lateral diffusion for these data, suggesting that meander is dominated by very large scale turbulence, even when considering travel times of 30-60 minutes.

20 DISTRIBUTION / AVAILABILITY OF ABSTRACT ☒ UNCLASSIFIED/UNLIMITED ☐ SAME AS RPT ☐ DTIC USERS	21 ABSTRACT SECURITY CLASSIFICATION UNCLASSIFIED
22a NAME OF RESPONSIBLE INDIVIDUAL Dr. P. Tag, contract monitor	22b TELEPHONE (Include Area Code) (408) 646-2927 — 22c OFFICE SYMBOL WU 6.2-31BG

DD FORM 1473, 84 MAR — 83 APR edition may be used until exhausted. All other editions are obsolete.

SECURITY CLASSIFICATION OF THIS PAGE

UNCLASSIFIED

CONTENTS

1. INTRODUCTION

The study of atmospheric diffusion can be simply defined as the investigation of the diluting effects of the atmosphere on a released contaminant. The atmosphere is most often in a turbulent state implying that its motions can be predicted only in a stochastic sense. Since virtually all gaseous pollutants and most airborne particulates very quickly become well mixed on the molecular level in the troposphere, diffusion of those materials can be described in a similar probabalistic manner. Introducing statistics automatically requires the user to consider the variations of those statistics in time and space. As an example of the later, a predicted crosswind concentration distribution represents only a first order approximation to the actual distribution, which will often show significant variations from that prediction. The study of those fluctuations is presently only beginning (see Sawford, 1985).

This study focuses on the time variations of diffusion statistics, specifically, the standard deviation of the crosswind concentration distribution (sigma-y). Skupniewicz and Schacher (1984b) have shown that overwater releases of material will diffuse in the crosswind (y) direction with two scales of motion. On one scale, material will disperse about the centerline of the plume or cloud due to turbulence of length scales close to the plume or cloud size. This scale of dispersion is referred to as relative dispersion, implying that the statistics can be observed by the motions of parcels relative to each other in a moving frame of reference. On the second and much larger scale, the plume or puff will disperse relative to a fixed axis, usually chosen to be the mean wind direction. Turbulence acts on the instantaneous plume or puff as if it were a single entity, and is referred to as single-particle diffusion. A more common and understandable synonym is meander.

Skupniewicz and Schacher (1984a) implicitly considered the combined diffusion properties of both components when hourly averaged plume parameterizations were derived from tracer experiments. In this report, the two components are separated in order to supply more information on the nature of the diffusion processes, and resultantly more knowledge of potential hazard from a contaminant release.

2. EXPANDED DATA BASE

Most descriptions of plume parameters rely on empirical formulae and/or major assumptions about the physical behavior of the atmosphere. Verification of these parameterizations therefore should utilize data gathered under a wide variety of atmospheric conditions and geographical locations. The Environmental Physics Group (EPG) at the Naval Postgraduate School (NPS) has made a significant effort to collect a diverse, overwater data base over a several year period for this purpose. These data are reported in Skupniewicz and Schacher (1984a) and will be hereafter referred to as the NPS data. The NPS data primarily consists of concentration profiles collected from an aircraft platform at various distances from a continuous surface release of SF_6 gas. Part of the work reported here was to integrate a new data set collected by the German Military Geophysical Office (GMGO) (see Groll et al, 1984) into our data base. These data were obtained in the North Sea via continuous SF_6 releases from a ship and subsequent downwind plume transects with a second ship sampling gas concentrations. Table 1 lists information on the three experiments made available to EPG.

Experiment Data	No. of Sampling Boats	No. of Plume Transects
23 May-06 Sep 79	3	516
14 Apr-29 Apr 80	4	558
04 Nov-13 Nov 80	4	260

Table 1. GMGO overwater tracer experiments available at EPG-NPS. Each transect produces an "instantaneous" sigma-y value used in this analysis.

Task I specifically involved several steps needed to produce plume parameters from the GMGO data:

1) transferring original 9-track data files to mass storage files in IBM 3033 readable format,
2) combining half-hour average meteorological files with nearly coincident tracer profiles, and
3) calculating the second moment of the concentration distribution (sigma-y) for each profile and the downwind distance from navigational information.

Table 2 lists the resulting data set contents and format.

VARIABLE	DEFINITION	UNITS	FORMAT
DATE	day, month, year	no units	3I2
TIME	hour	Z	I4
RH	relative humidity	%	F5.1
WD	wind direction	deg	I4
DB17	dry bulb at 17m	C	F5.1
WSM	wind speed (MET)	m/s	F5.2
WB17	wet bulb at 17m	C	F5.1
ET	water temperature	C	F5.1
DB3	dry bulb at 3m	C	F5.1
WB3	wet bulb at 3m	C	F5.1
GRAD	gradient	C/1000m	I4
SB	speed of boat	m/s	F5.2
SS	source strength	m^3/hr	F2.0
SH	sampling height	m	I2
WSS	wind speed (SF6)	m/s	F5.2
DS	distance from source	m	F8.1
BTS	bearing toward source	deg	F5.0
HD	heading	deg	F2.0
# pt	no. of points used for CWCI	no units	I2
CWCI	cross wind concentration integration	ppb-m	F8.0
MEAN	mean mass position	m	F6.1
SD	standard deviation	m	F6.1

Table 2. Contents of new GMGO overwater tracer data set added to the EPG overwater data base. Format is in FORTRAN code. Public mass storage data set name is "MSS.F3896.DATA.NEWSM".

3. RELATIVE DIFFUSION PARAMETERIZATION

The basic approach used in parameterizing the relative diffusion is to group observations according to Pasquill-Gifford equivalent stability classes (see Turner, 1967), and then regress sigma-y versus range (from the release point) for each class. Sigma-y was defined in the last section as the second moment of the concentration distribution for a given profile. The customary assumption that concentration in the y direction is independent of concentration in either the x or z direction leads to the conclusion that these instantaneous "snapshots" of the SF6 plume are identical to the crosswind dimensions of a hypothetical "puff" or "burst" release under the same atmospheric conditions.

The methodology for determining stability class is described in detail in Skupniewicz and Schacher (1984a). Briefly, the scheme uses windspeed, air-sea temperature differences and relative humidity to produce stability classes equivalent to the well-known Pasquill-Gifford diffusion categories. [Whether a true equivalence exists is a matter of controversy and is discussed in Skupniewicz and Schacher (1984a).]
Under this scheme classes are assigned a letter designating atmospheric stability, with "B" representing the most unstable situations, "C" representing moderately unstable, "D" representing neutral, and "E" representing moderately stable conditions.

After dividing the data according to stability, the subsets were examined for dependence upon wind speed, time of day, and day to day trends. No obvious dependences were found. Figures

1-3 show sigma-y vs. downwind distance, with the integer truncation of the wind speed used as the point designator. In as much as windspeed gives a first order approximation to sea-state, increased surface stress within a given stability class has a negligible effect on diffusion. This result is particularly surprising for the neutral case (class D), where a small air-sea temperature difference will always produce neutral stability under this scheme regardless of windspeed. Intuitively, one would expect that higher windspeed would enhance the plume spread. Because stable or unstable profiles tend towards neutrality as windspeed increases in this stability scheme, windspeed dependence is not expected in non-neutral categories. It is also noteworthy that stable situations are found exclusively in light wind situations in the North Sea experiments. These situations were not found in the California experiments.

Based on the above data, the parameterization chosen for relative diffusion is a simple linear relationship. The following factors influenced this choice. Instantaneous releases into a turbulent atmosphere will theoretically experience the following four different growth regimes:

a) the initial stage

b) the inertial stage

c) the central stage

d) the final stage

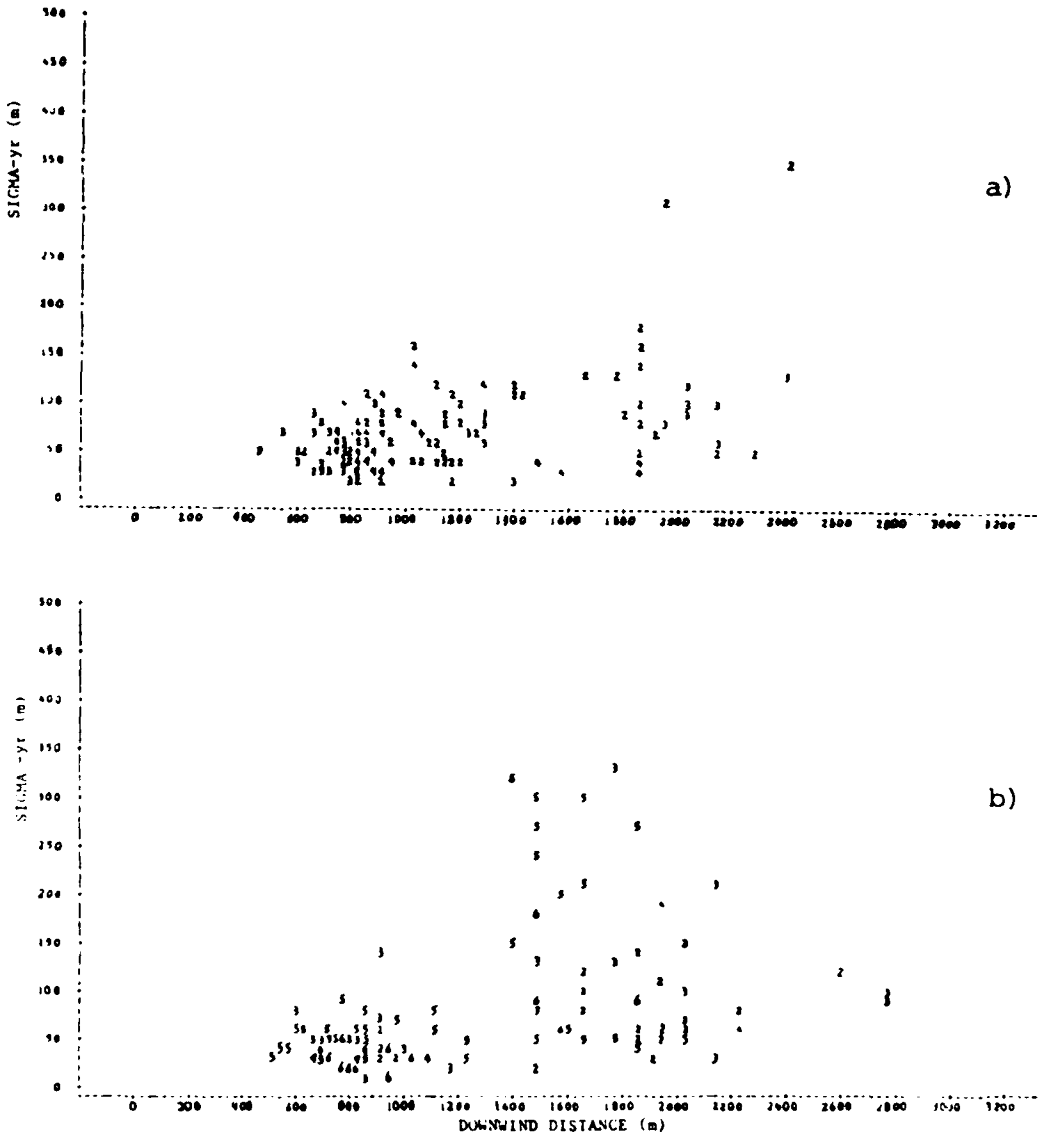

Figure 1. Sigma-y relative vs. downwind distance. Symbol of data point is integer truncation of windspeed in m/s. Only data 3200 m from source is plotted.
a) Pasquill-Gifford stability class B (moderately unstable), GMGO data. 23 data points are hidden.
b) Pasquill-Gifford stability class C (slightly unstable), GMGO data. 15 data points hidden, 1 data point missing.

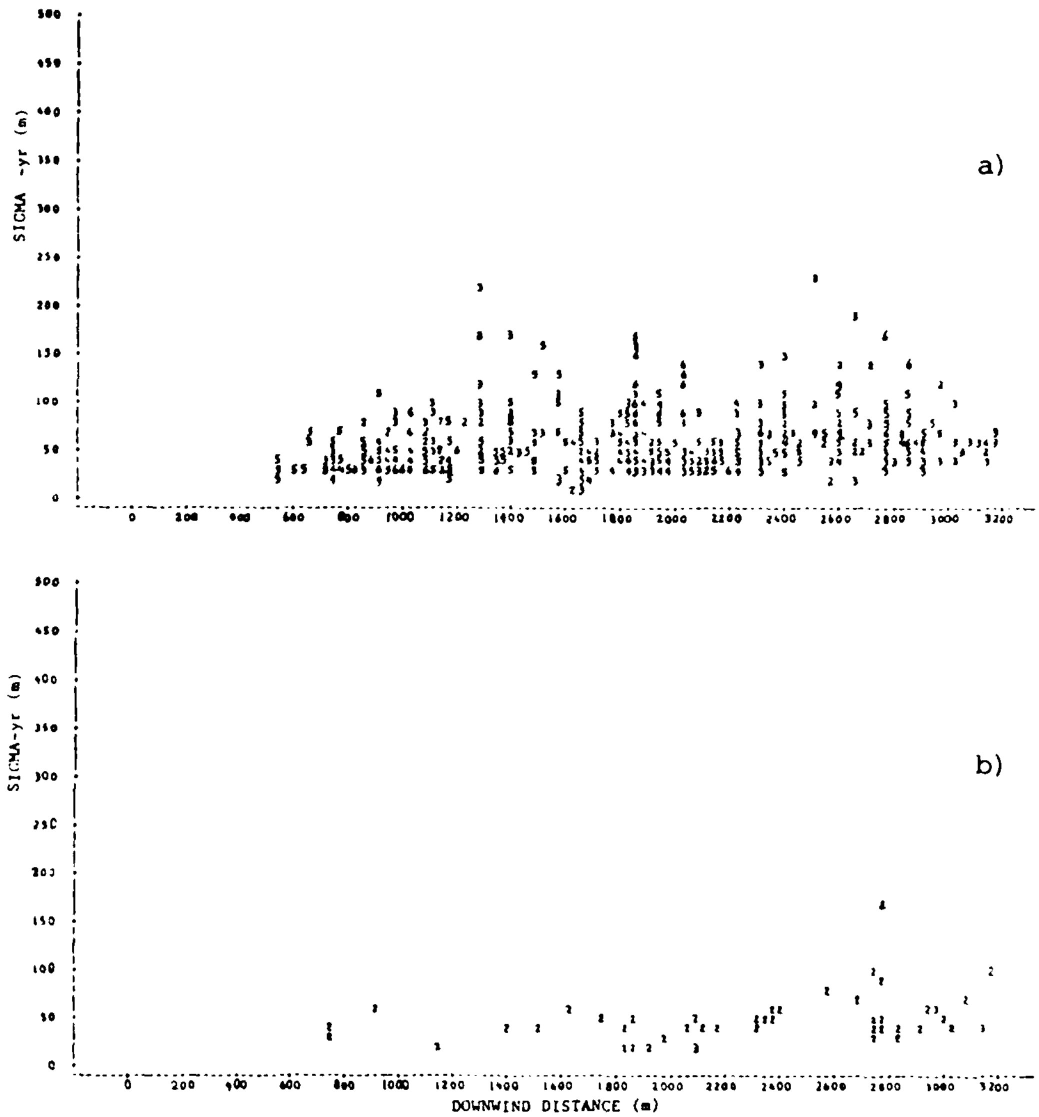

Figure 2. Same as figure 1, except a) Pasquill-Gifford stability class D (neutral), GMGO data. 194 data points hidden, 114 data points missing. b) class E (slightly stable), GMGO data. 8 data points hidden, 153 data points missing.

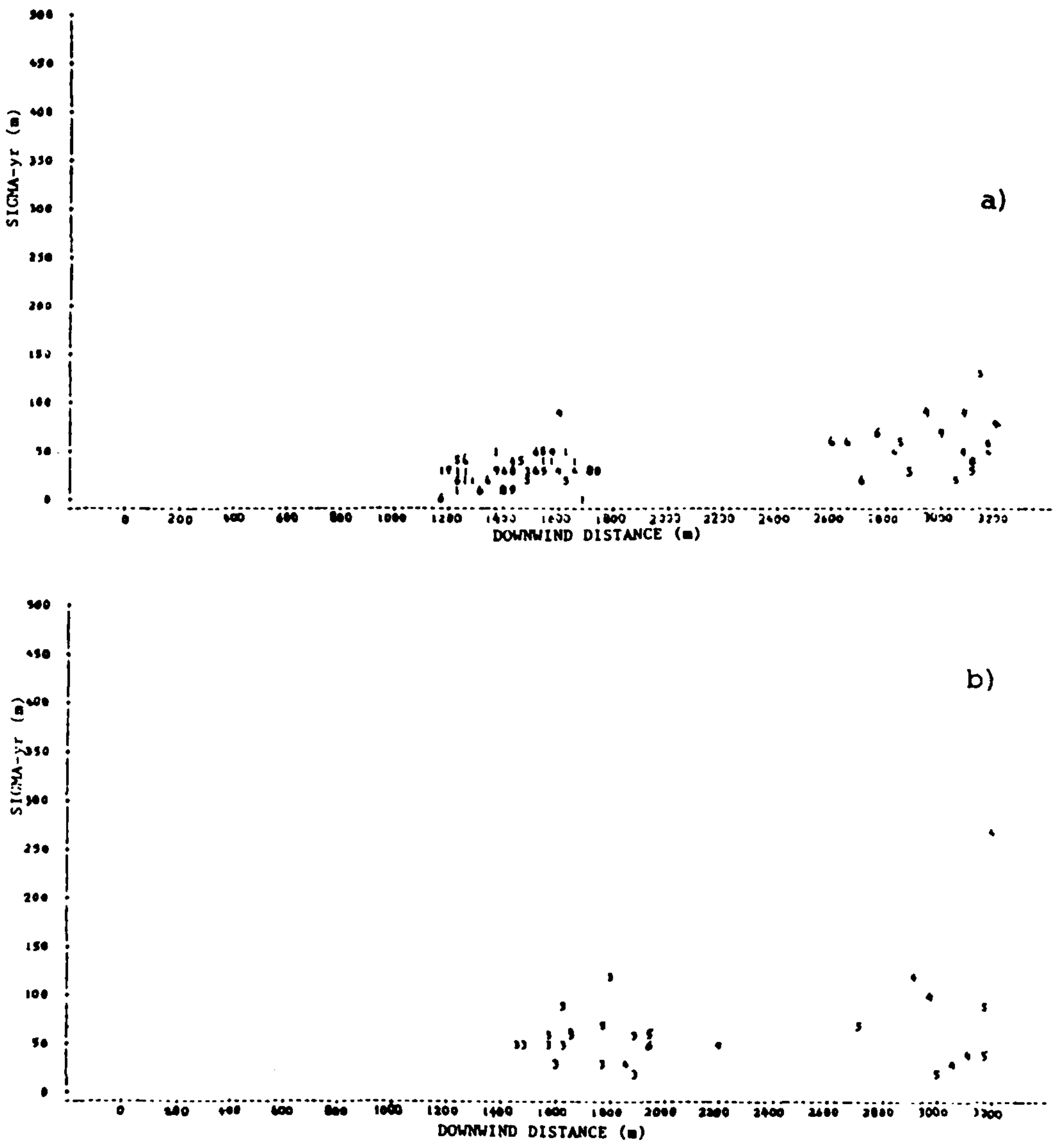

Figure 3. Same as figure 1, except a) Pasquill-Gifford stability class D (neutral), NPS data. 13 data points hidden, 145 data points missing. b) class E (slightly stable), NPS data. 1 data point hidden, 45 data points missing.

The initial stage applies to distances of only 10-100m. The inertial stage will be relevent from 100m to less than 1km. The central stage will apply from 1km to 10km and the final stage will apply thereafter. These bounds are highly variable.

The initial stage of growth is valid when the instantaneous puff "remembers" its initial size. In this regime cloud size will increase linearly with distance or travel time because each particle in the cloud will move with its initial velocity and the particles have not had time enough to become correlated with each other.

The initial stage is followed by growth dominated by turbulence in the inertial subrange. In the inertial region, plume growth can be shown to follow

$$\sigma_{yr}^2 = a\varepsilon t^3 , \tag{1}$$

where σ_{yr} is the relative sigma-y,

a is a constant,

ε is the turbulent kinetic energy dissipation rate, and

t is travel time of the cloud.

This inertial stage of growth is valid only where the width of the cloud is small compared to the average height of the cloud; surface-released clouds seldom meet this criterium.

Smith and Hay (1961) laid the foundation for considering cloud spread as a function of turbulent energy in a "sliding" spectral window. They found both experimentally and theoretically that cloud spread will approximately follow a linear growth relationship

$$\sigma_{yr} = 0.22\ ix \ , \tag{2}$$

where i is the total turbulence intensity, and

$$i = \frac{(\langle u^2 + v^2 + w^2 \rangle)^{1/2}}{U} \ , \tag{3}$$

where x is downwind distance,

u,v,w are fluctuating wind components, and

U is mean windspeed.

Mikkelsen and Eckman (1984) have recently given support to these results from overland experiments for surface releases in short to medium ranges.

At long distances from the source, correlation between hypothetical particles within the cloud approaches zero, and the spread of the cloud will behave like the asymptotic single-particle solution,

$$\sigma_{yr} \propto t^{1/2} \tag{4}$$

Large scale motions, however, are often organized into coherent vortex structures (i.e. cyclones). As a result, this limit is rarely reached, and growth continues along a more or less linear asymptote.

All of these above arguments and the rather linear shape of the data scatter lead us to a linear paramterization. The results are shown in figures 4-6 and summarized in table 3. Note that there is very little unstable data at ranges greater than 3000m. This is primarily due to the fact that, under these conditions, diffusion is enhanced and tracer concentrations are greatly reduced far from the source. This makes the plume difficult to locate, and may bias measurements towards narrow, concentrated profiles. The most striking feature is that there is no clear distinction between P-G classes B and C (GMGO data), or between classes D and E (both data sets). Those pairs are so closely matched that we suggest only a two-class parameterization (also shown in table 3); one for all unstable conditions and a second for neutral to stable stratification. While turbulence intensity is not explicitly used in the paramterization, this two-class system is supported by the calculated wind variances from the NPS data shown in table 4. These wind data include some measurements from periods not coincident with tracer releases, and do not include some periods when tracers were released. Nonetheless, the largest change in turbulence (when moving from one to an adjacent category) occurs between class D and class C.

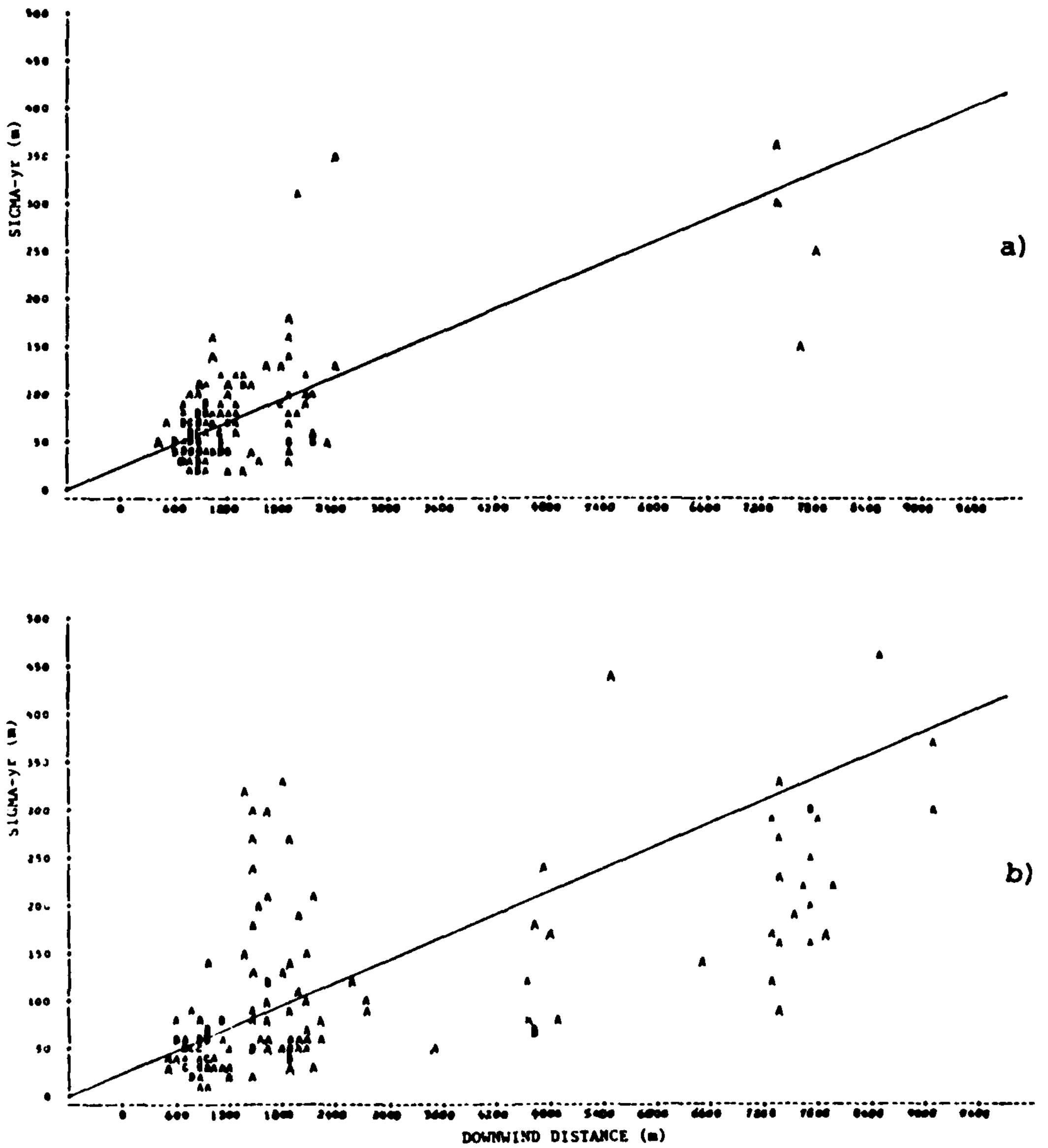

Figure 4. Sigma-y relative vs. downwind distance with solid line representing the recommended parameterization of table 3. Symbol A represents one data point, B represents two data points, etc. Same data as figure 1, except long range data is included. Data is a) Pasquill-Gifford stability class B, GMGO data, and b) class C, GMGO data.

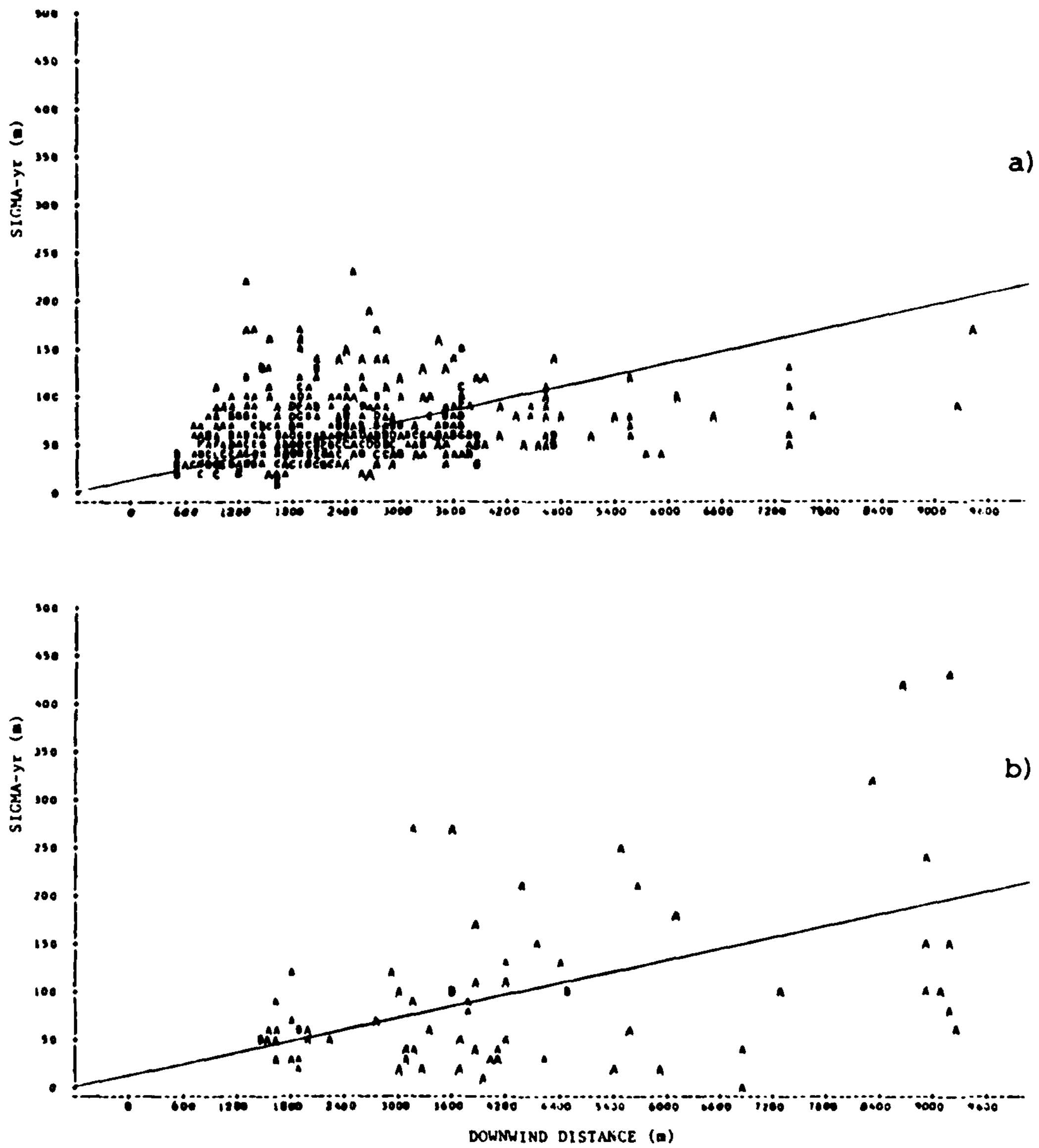

Figure 5. Same as figure 4, except a) Pasquill-Gifford stability class D, GMGO data, and b) class E, GMGO data.

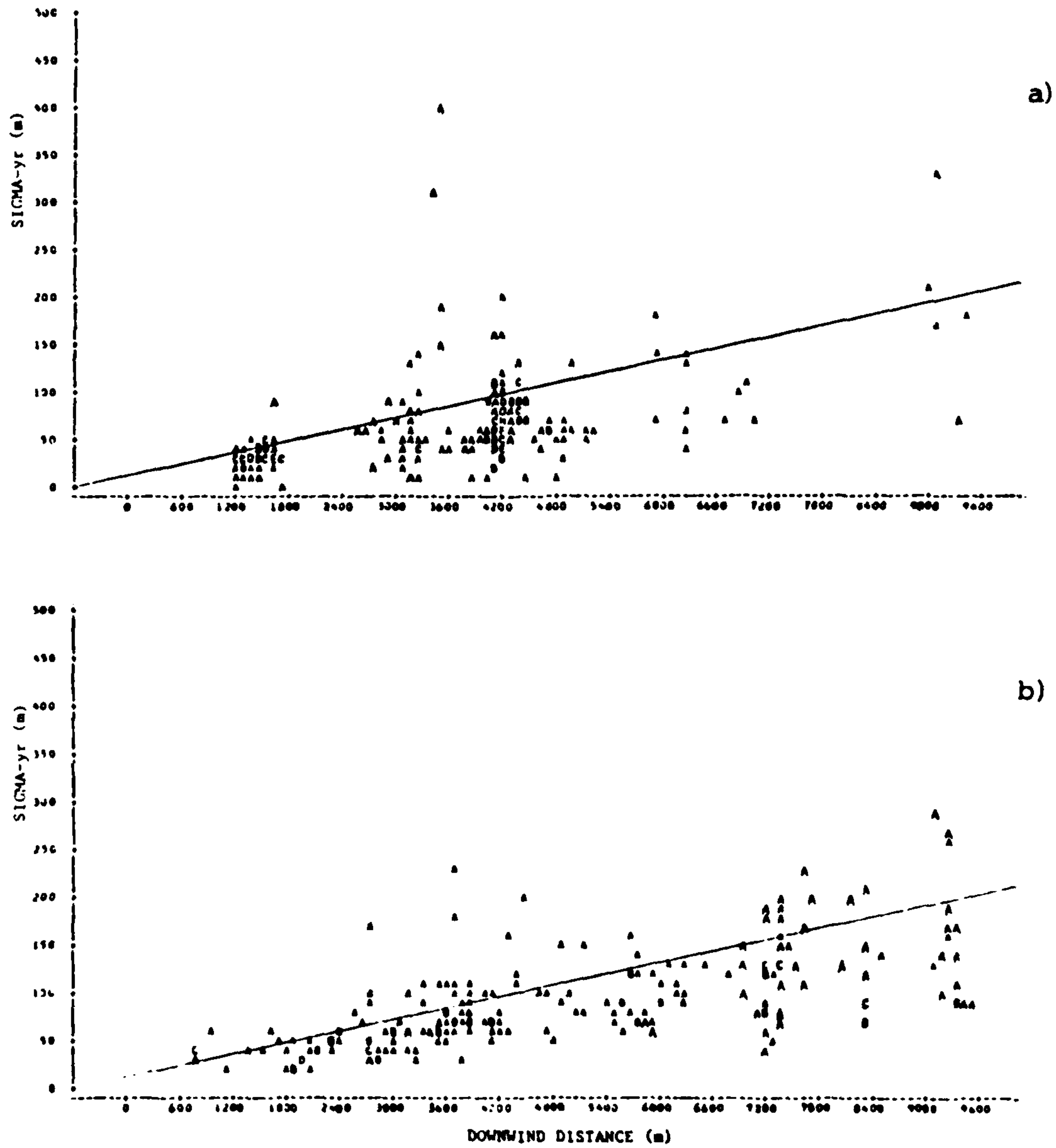

Figure 6. Same as figure 4, except a) Pasquill-Gifford stability class D, NPS data, and b) class E, NPS data.

DATA	PASQUILL-GIFFORD CLASS	SLOPE	#POINTS
GMGO	B	.0467	132
GMGO	C	.0357	140
GMGO	D	.0227	603
GMGO	E	.0178	206
NPS	D	.0178	215
NPS	E	.0228	72
GMGO	B+C **	.0410	272
GMGO + NPS	D+E **	.0211	1096

**Last 2 rows are suggested values.

Table 3. Relative diffusion parameterization for overwater, surface, medium range (1-12km) releases. Slopes are least squared linear regression to data. Sigma-y relative = (Slope)x(downwind distance).

Pasquill-Gifford Stability Class	Sigma Wind Direction (deg) 1 min ave	10 min ave	# Hours Of Data
B	3.96	6.41	7
C	2.95	4.59	11
D	1.82	2.92	114
E	1.32	2.61	11

Table 4. Sigma theta as a function of P-G stability class. Sampling rate is 1 Hz. Data is from NPS experiments.

This two-class feature can also qualitively seen in figure 7 where turbulence intensity as a function of stability (defined using the Monin-Obuknov length [L]) was plotted by Schacher et al (1982). These data show a step increase in sigma theta (turbulence intensity) for the 1 minute averages at roughly L = -40m. 1 hour averages are also plotted for a comparison, even though 1 minute averages are much more applicable to relative diffusion in these experiments. Note that the 1 hour values do not show this effect and are 4 to 5 times larger than 1 minute values. This suggests that our two-class approach may break down as the cloud travel time increases. We therefore do not recommend interpolating our results to distances greater than 10 km.

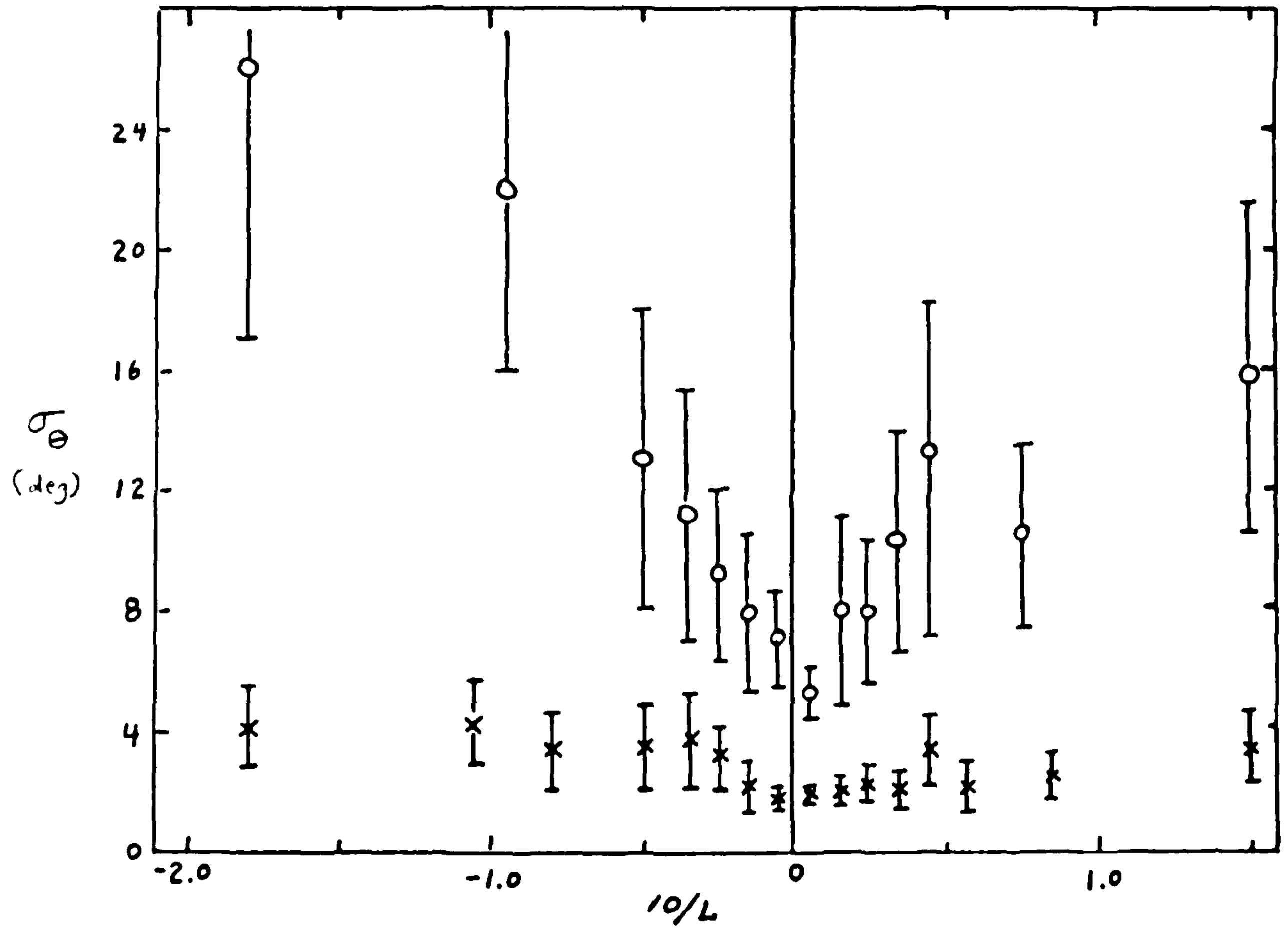

Figure 7. Wind direction sigma (sigma theta) vs. z/L (z is the height, 10m, and L is the Monin-Obukhov length). X's are 1 min averages, and O's are 1 hr averages. Data is from NPS. (see Schacher, et al., 1982)

4. MEANDER (SINGLE PARTICLE) PARAMETERIZATION

For purposes of describing meander, information on the motion of the plume is available only from the NPS data set. Meander was measured by calculating the distance between the center of mass for a given profile and the axis defined by the mean wind vector. The method used to calculate the mean wind vector was crucial. After experimenting with various techniques, we decided to let the average travel time of the plume define the proper averaging period for the vector; this travel time was roughly one-half hour. Since the wind was measured only at the release point, tracer profiles were correlated with average wind vectors in half-hour bins offset by 15 minutes to account for plume transport.

The NPS experiment was designed so that the plume was sampled at nearly discrete ranges from the release point. This sampling procedure allowed us to segregate data into range bins. The collection of off axis center of mass positions for a given range bin represents a probability distribution for the meander of a plume or puff. Each experimental day produced several distributions at various downwind distances from the source. The distributions were then analyzed for normality, and the standard deviations (which represent sigma-y due to meander) were determined.

The data were examined for dependence on windspeed, stability class, inversion height, experimental day, and time of day. The day to day variability was so large that it tended to swamp other dependencies. Figures 8-21 show day by day plots of the center of mass distributions interlaced with the respective wind direction time histories and spectral plots.

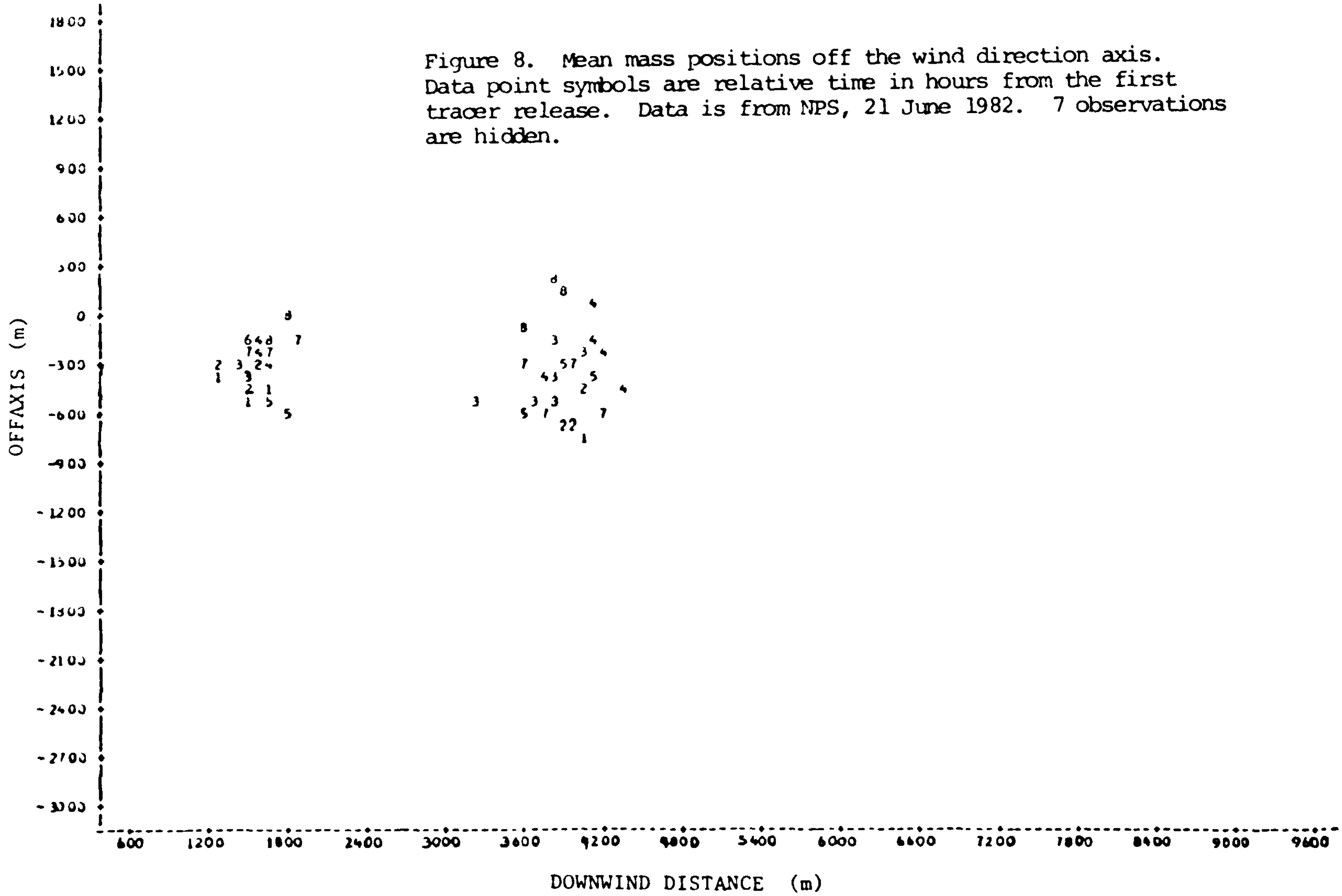

Figure 8. Mean mass positions off the wind direction axis. Data point symbols are relative time in hours from the first tracer release. Data is from NPS, 21 June 1982. 7 observations are hidden.

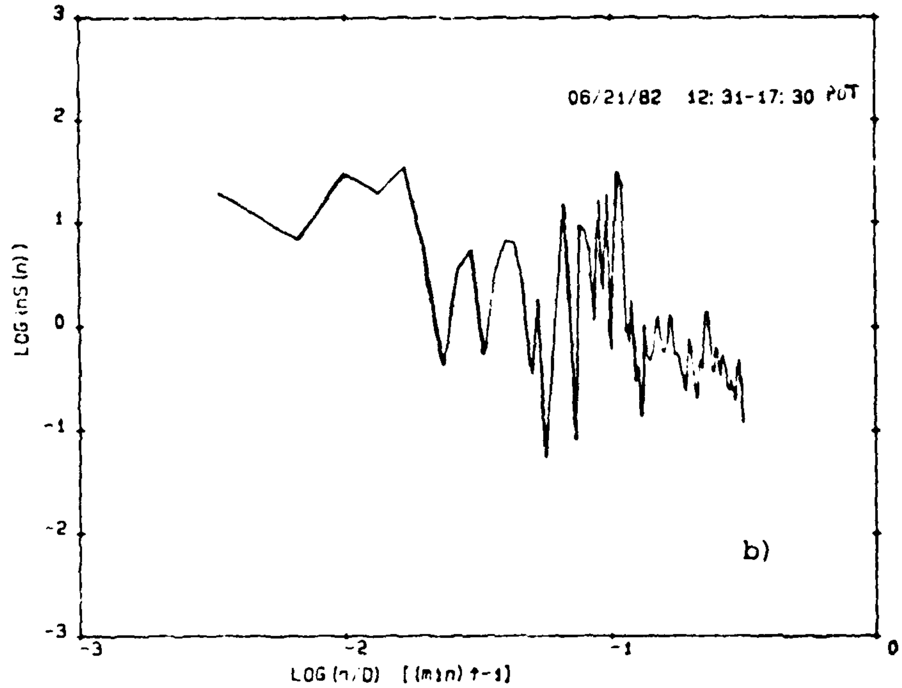

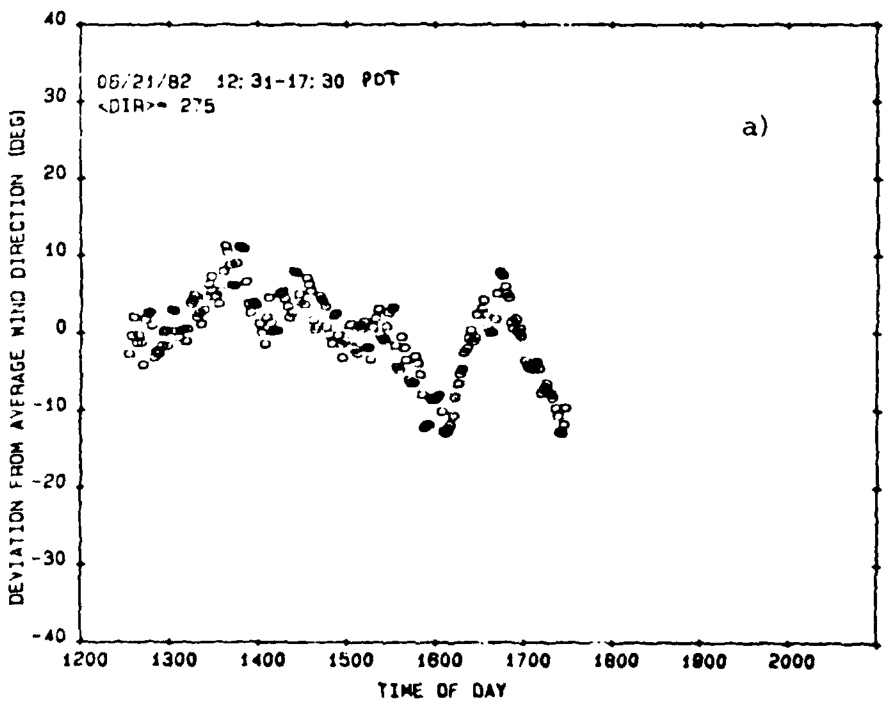

Figure 9. a) Wind direction time series, and b) power spectra for tracer release depicted in figure 8. Time series data are 2 minute averages of wind direction sampled at 1 Hz. Spectral points are smoothed with a 5% sliding average. S(n) is wind direction power spectral density at frequency n. D is the total sampling time. <DIR> is the mean wind direction.

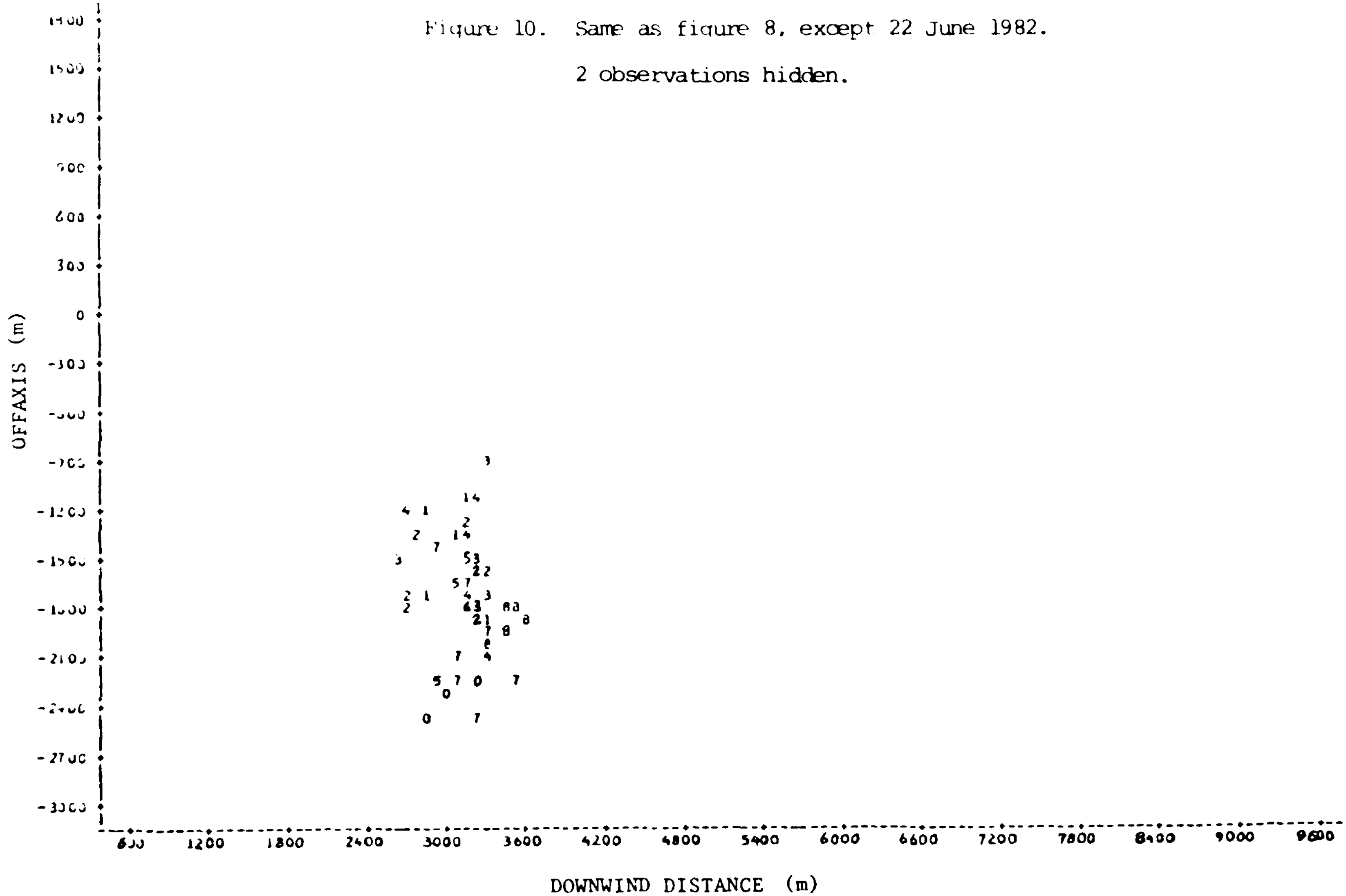

Figure 10. Same as figure 8, except 22 June 1982.

2 observations hidden.

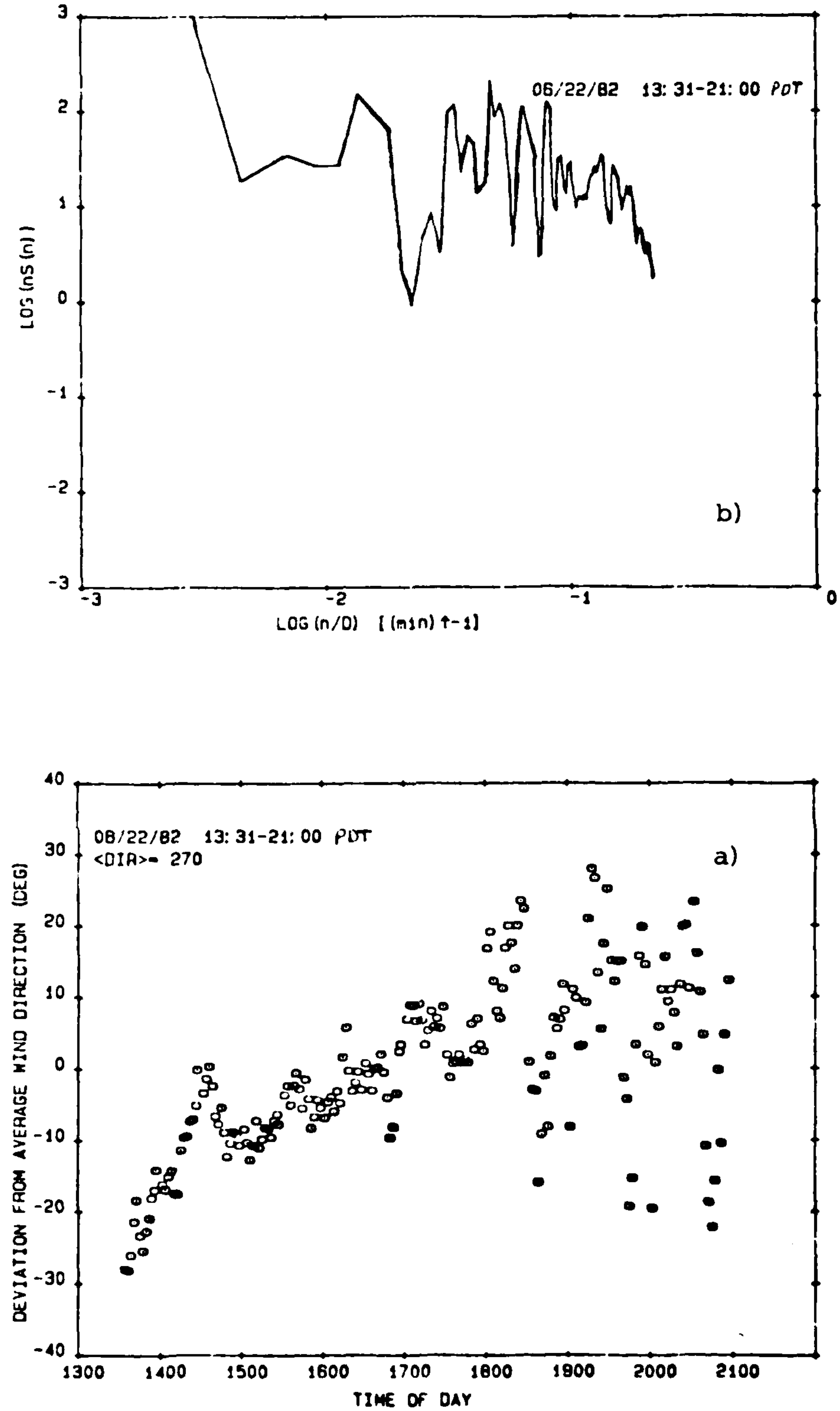

Figure 11. a) Wind direction time series, and b) power spectra for tracer release depicted in figure 10.

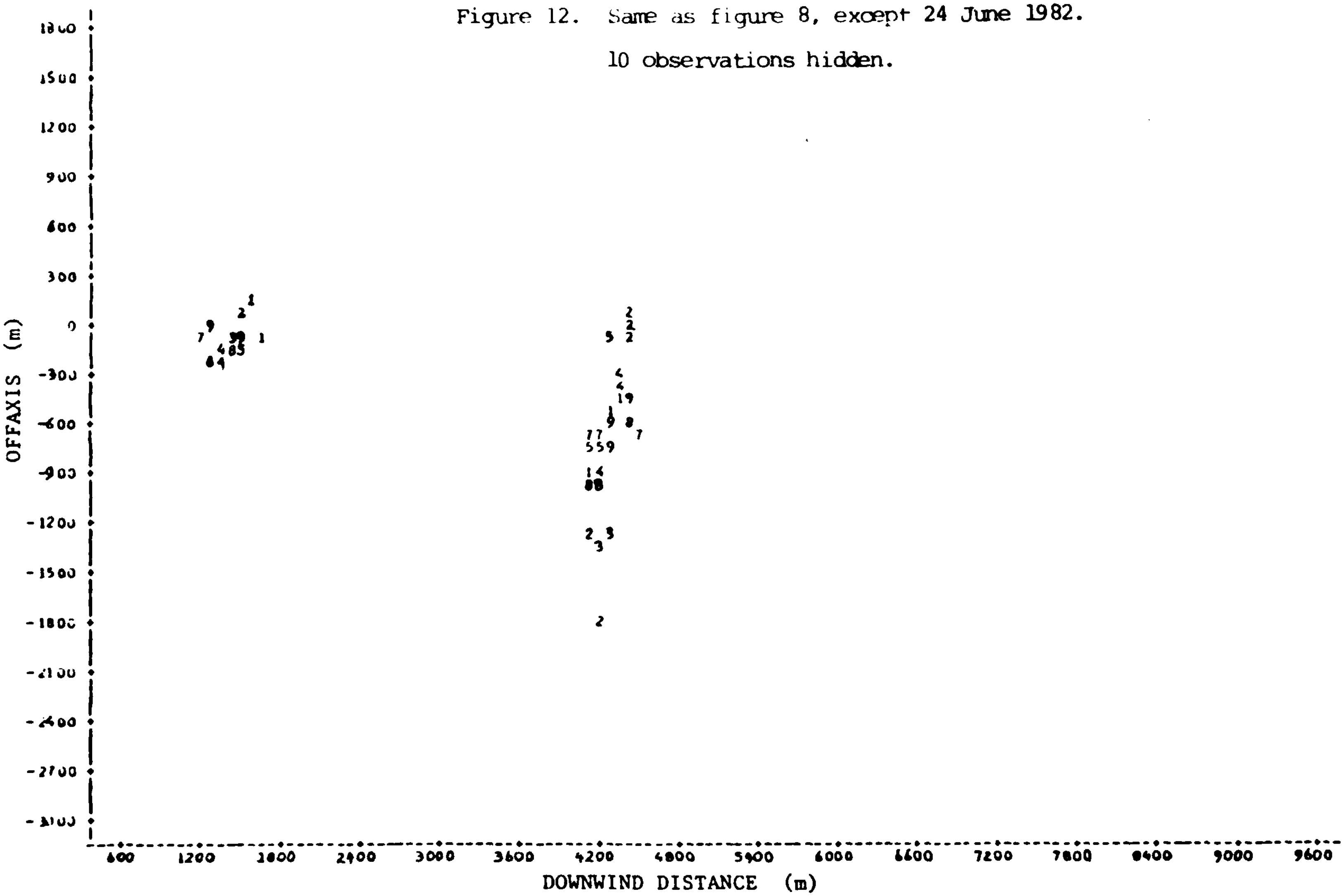

Figure 12. Same as figure 8, except 24 June 1982.

10 observations hidden.

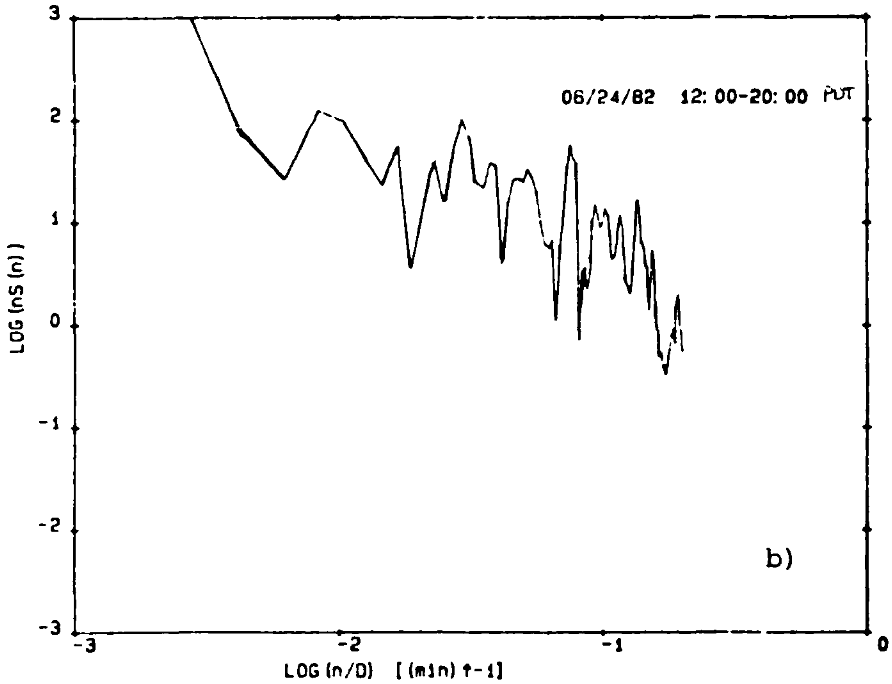

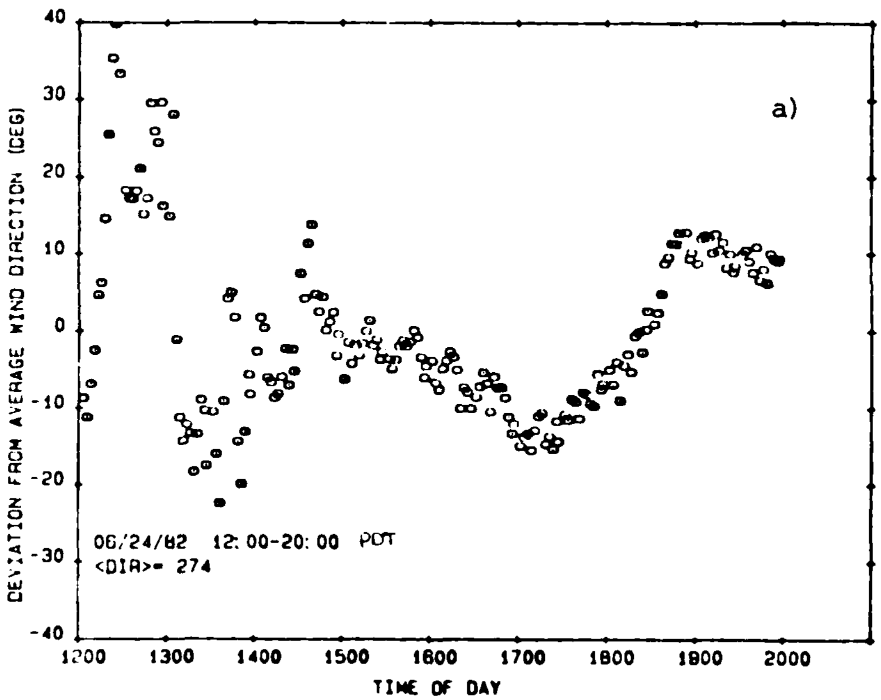

Figure 13. a) Wind direction time series, and b) power spectra for tracer release depicted in figure 12.

Figure 14. Same as figure 8, except 25 June 1982.

25 observations hidden.

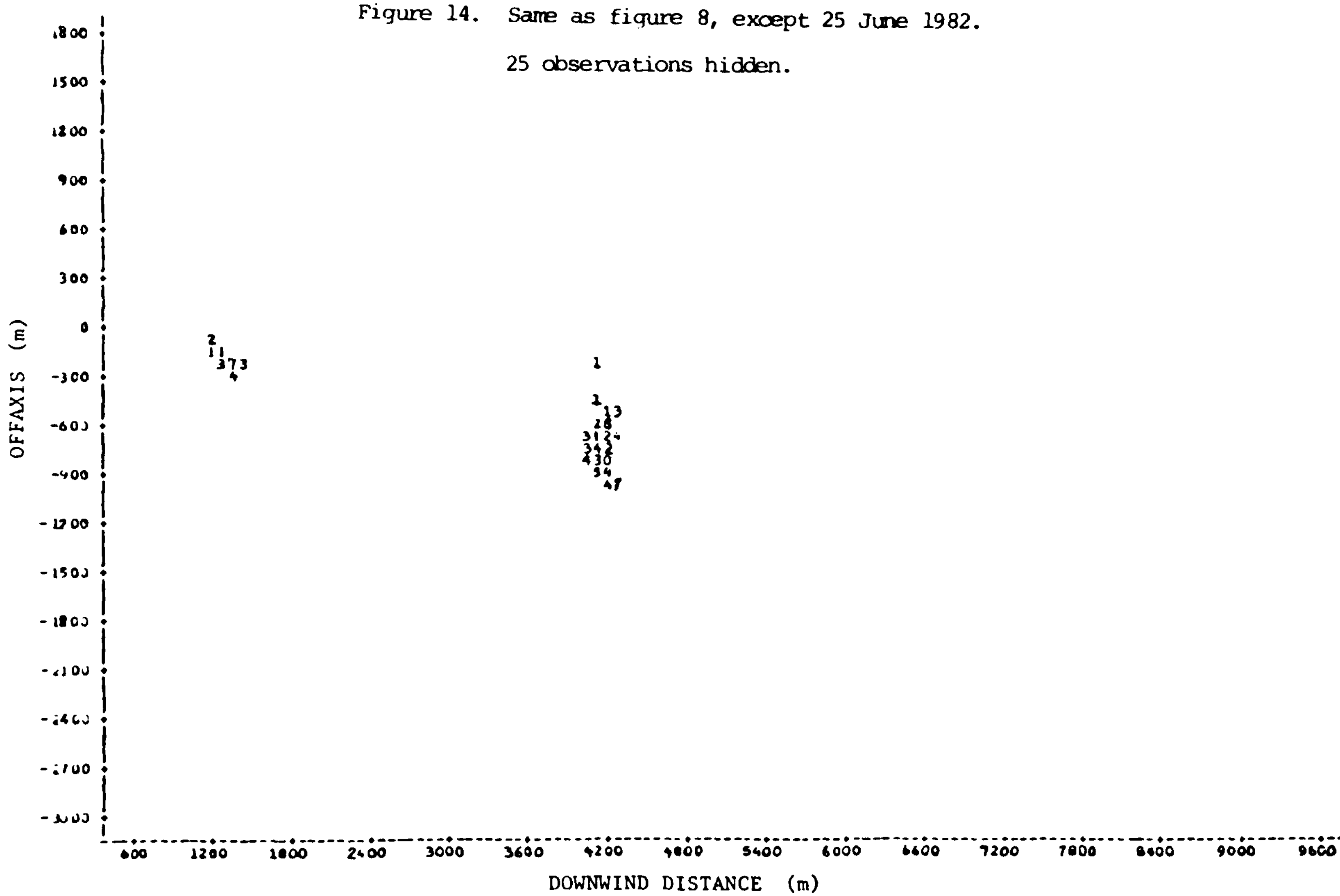

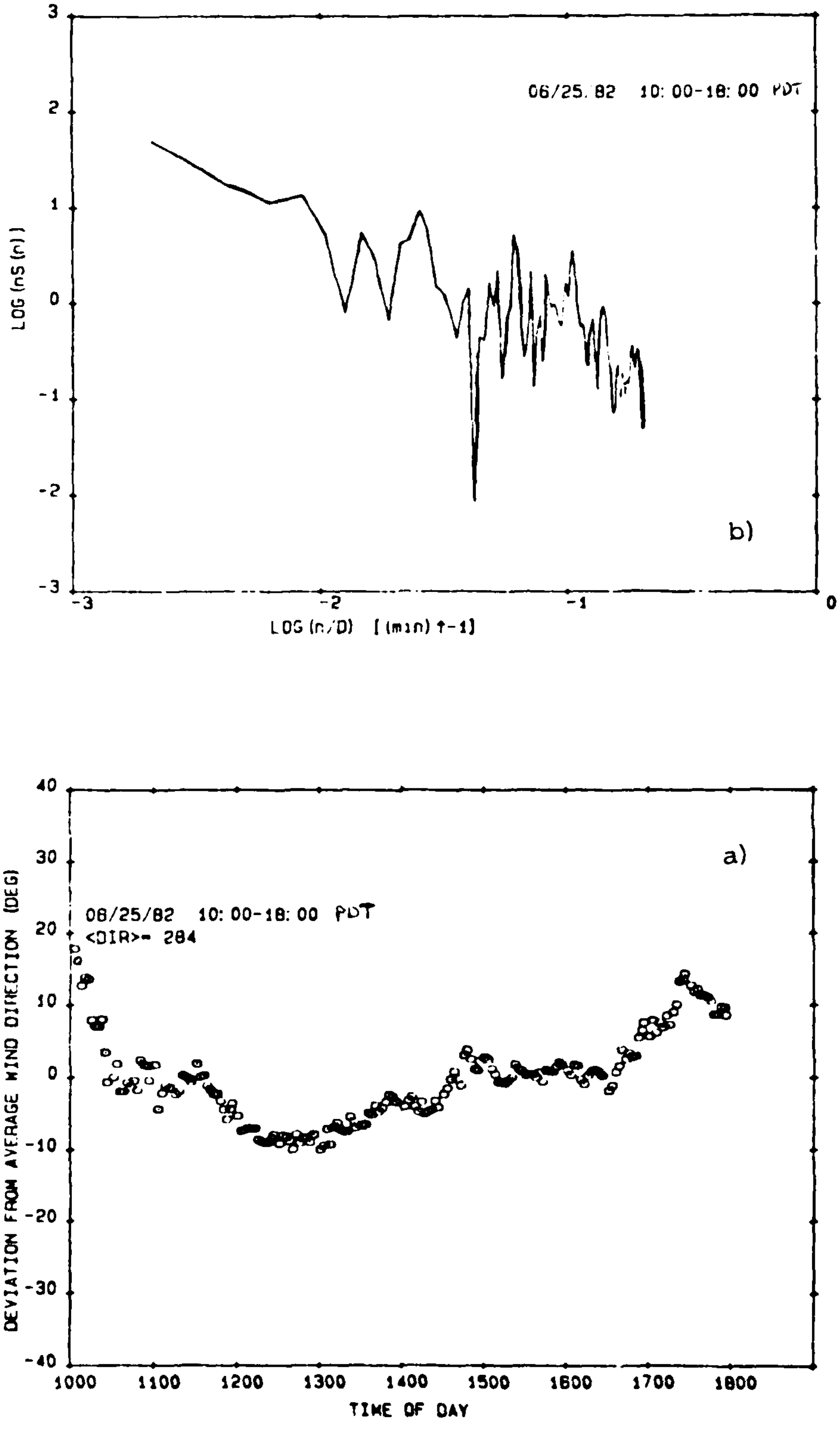

Figure 15. a) Wind direction time series, and b) power spectra for tracer release depicted in figure 14.

Figure 16. Same as figure 8, except 27 June 1982. 2 observations hidden.

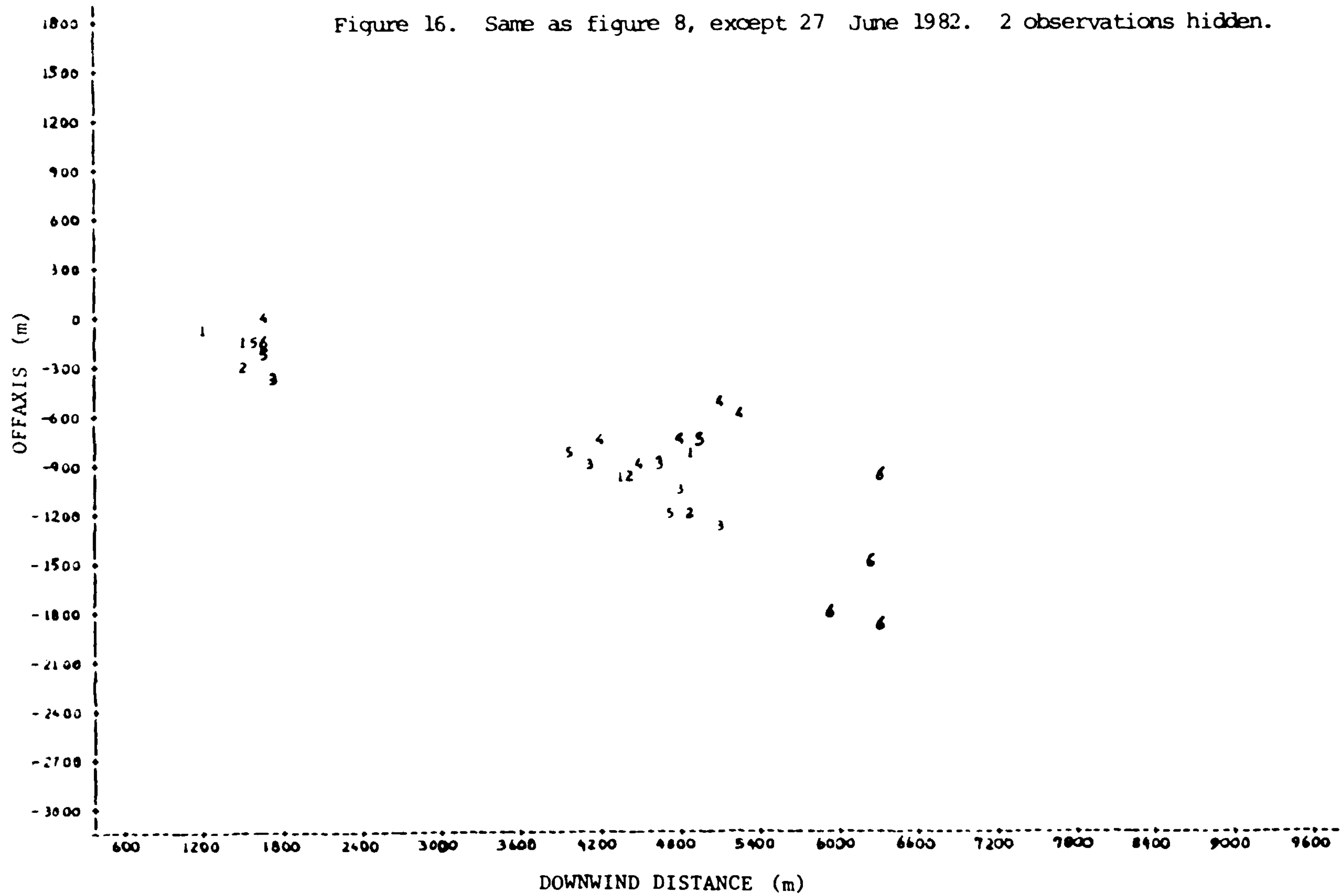

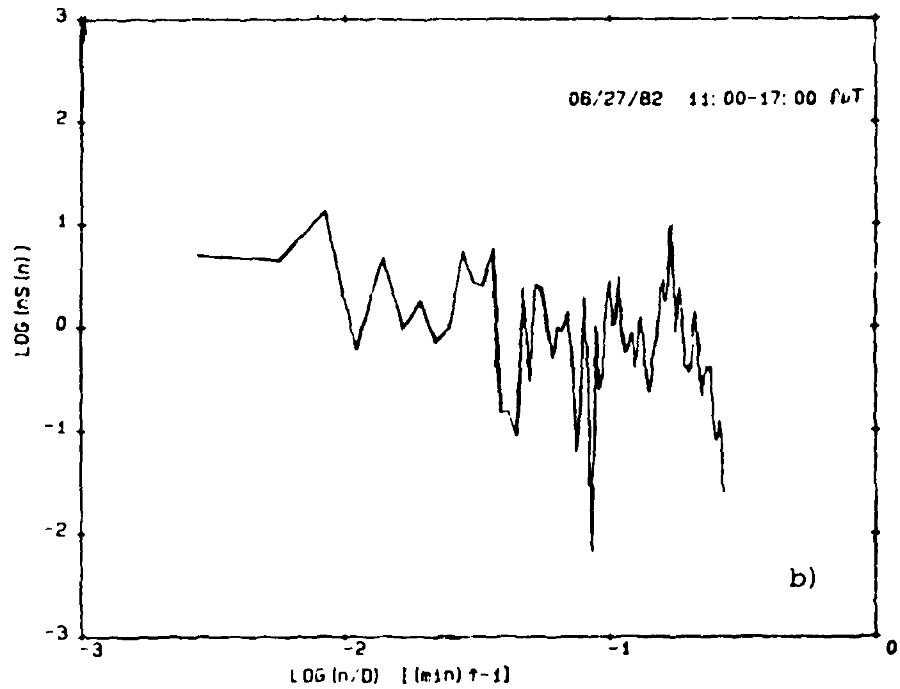

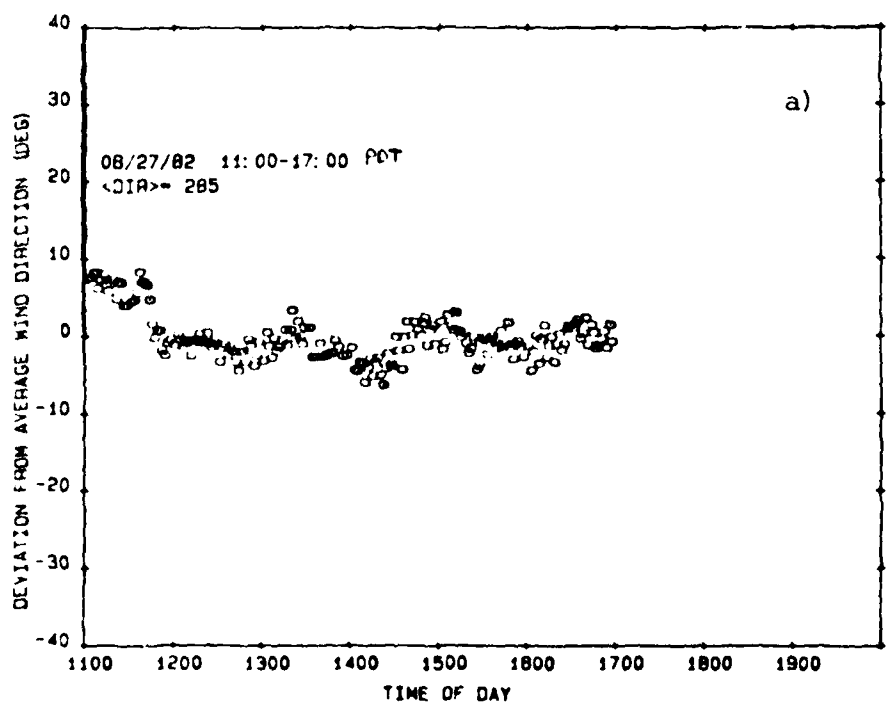

Figure 17. a) Wind direction time series, and b) power spectra for tracer release depicted in figure 16.

Figure 18. Same as figure 8, except 28 June 1982.

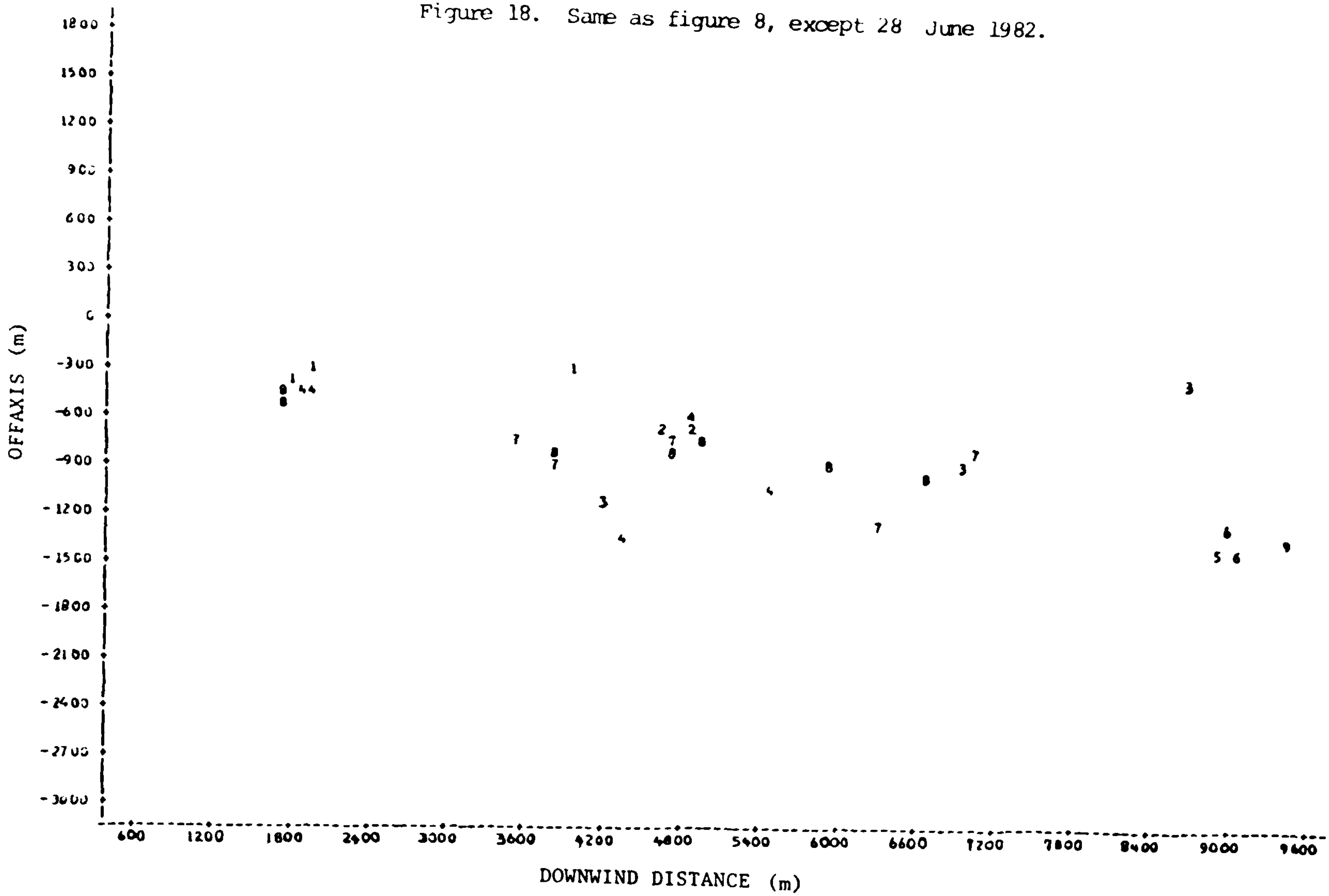

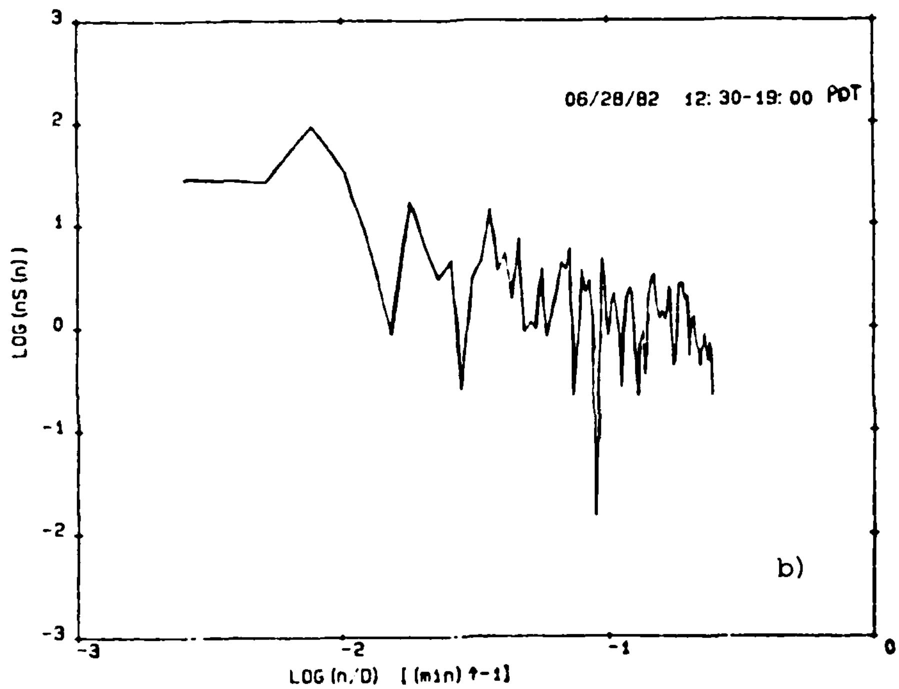

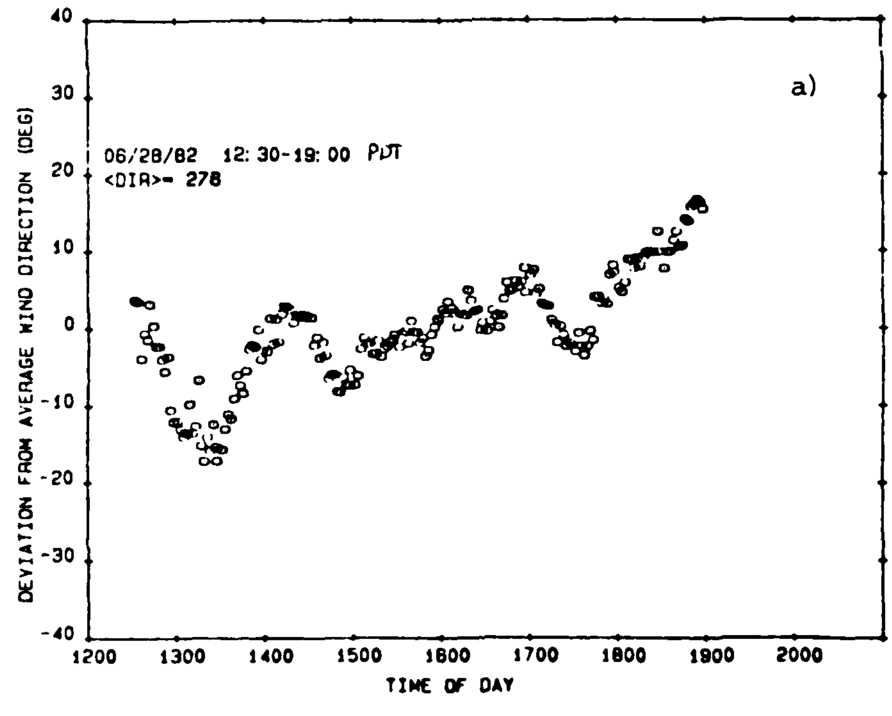

Figure 19. a) Wind direction time series, and b) power spectra for tracer release depicted in figure 18.

Figure 20. Same as figure 8, except 29 June 1982.

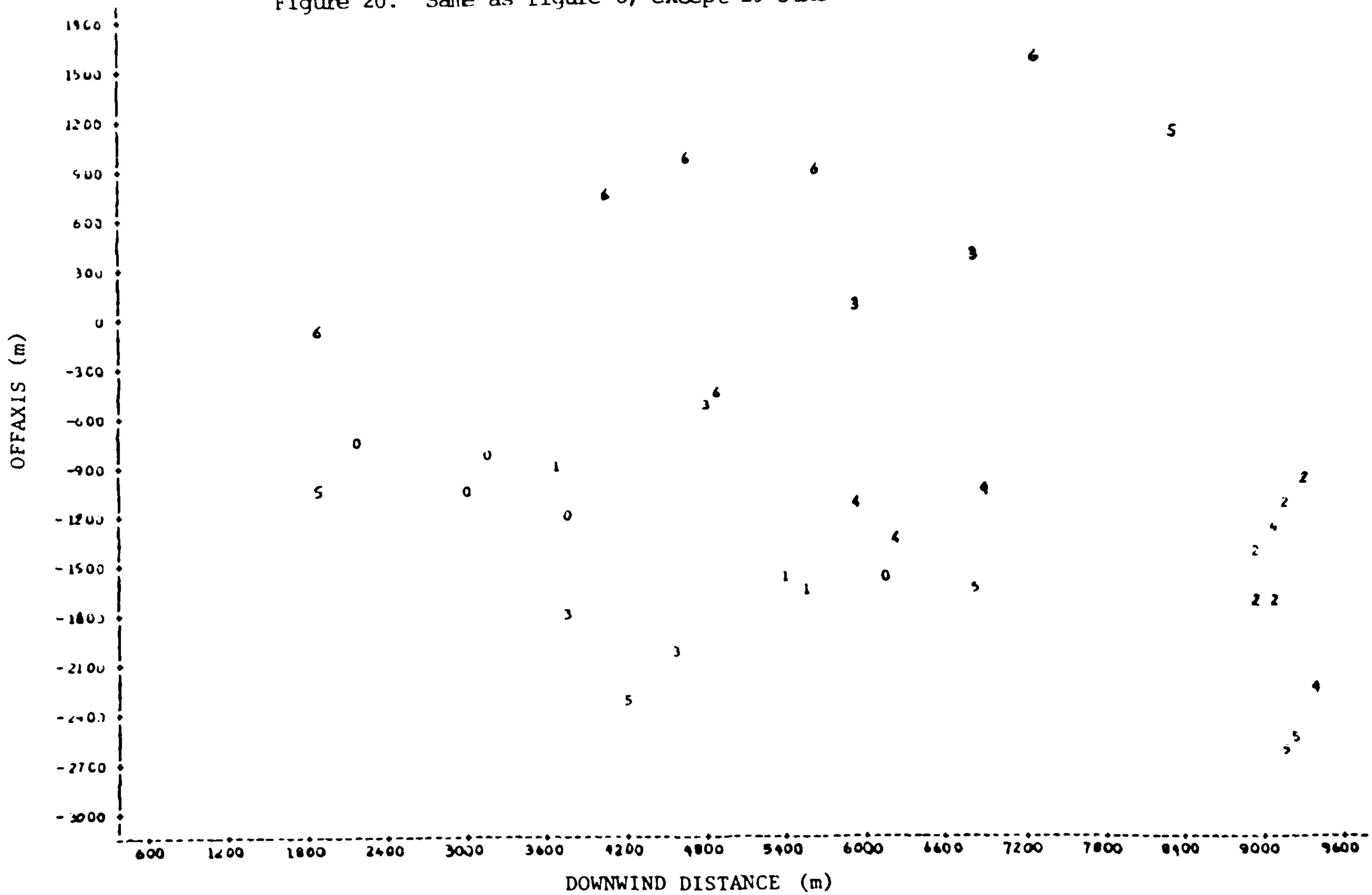

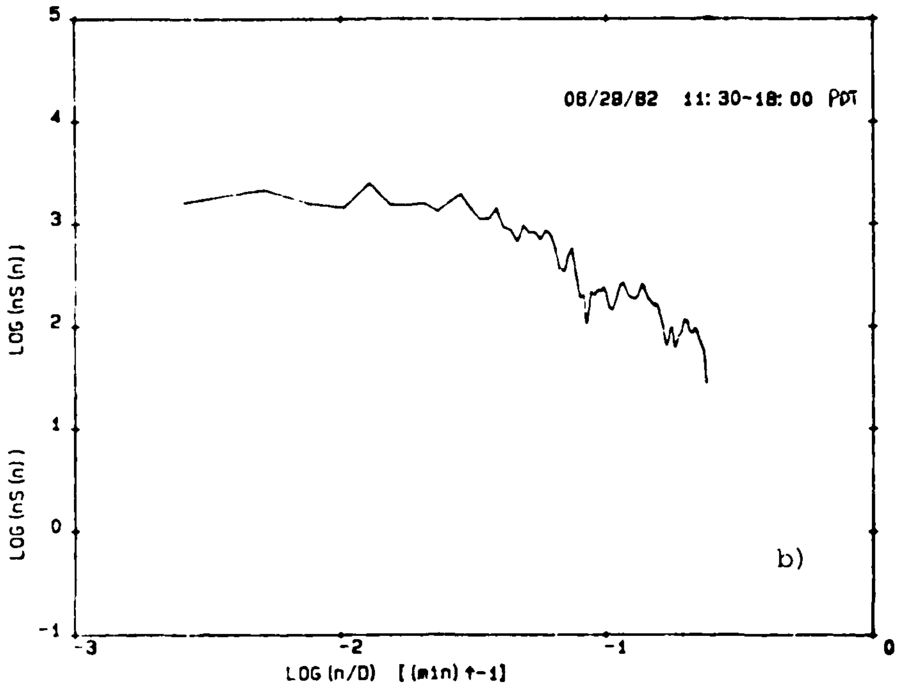

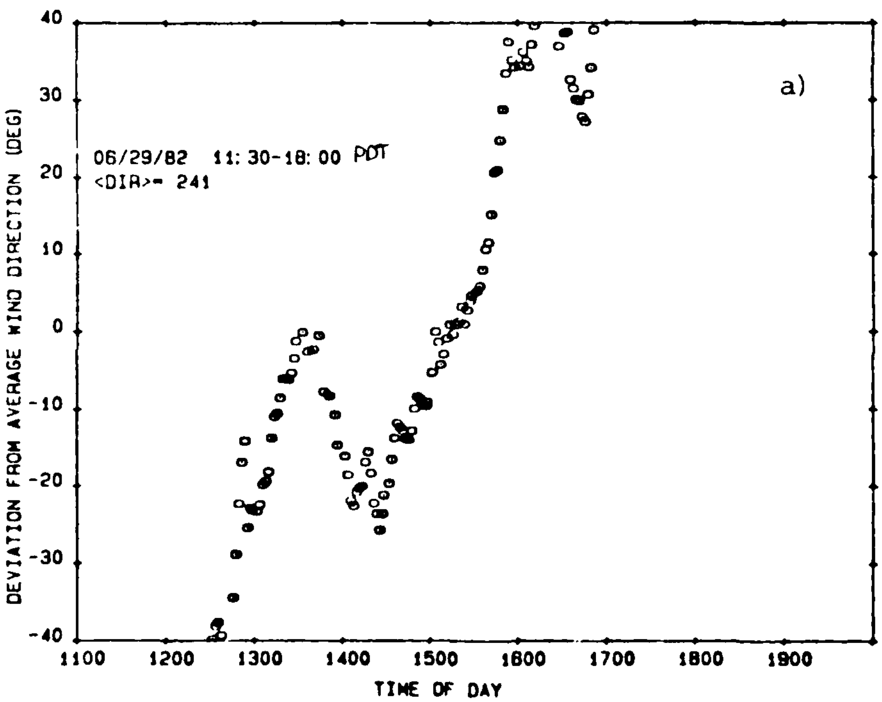

Figure 21. a) Wind direction time series, and b) power spectra for tracer release depicted in figure 20.

Individual data points are marked with integer values of the measurement hour for a given experimental day. Note that the mean position of the cluster often moves off the centerline, but data are distributed evenly over the course of a day. Large variations in the meander "envelope" can be seen from day to day, and the wind direction time series differ radically. The power spectra also vary greatly from day to day. Spectral parameters are summarized in table 5. Spectral gaps (defined in the table 5 caption) exist in most situations, with slopes of approximately -2 in the low frequency part of the spectra.
There appears to be no clear relationship between the total energy in the turbulent and low frequency parts of the spectra. Since meander is driven by the low frequency energy, this discourages attempts at parameterizations of meander based on surface layer scaling.

As stated above, center of mass distributions were grouped by experimental day and range bin. Variations of the position of the measurement aircraft dictated range bins to be 2 km long. Relevant statistics are given in table 6. Examination of the Shapiro-Wilk statistics (Shapiro and Wilk, 1965) indicates that the crosswind distributions are represented fairly well by normal distributions. This suggests that Gaussian models will be valid even for dispersion caused by meander, given the proper sigma-y.

Date	Classical[1] peak	Gap[2]	Slope[3]
6/21/82	10 min	20 min	-6.5/3
6/22/82	20	50	-7/3
6/24/82	30	50	-6.5/3
6/25/82	20	25	-6/3
6/27/82	5	15	-5.5/3
6/28/82	10	15	-5.5/3
6/29/82	?	?	?

1 Classical peak is the inverse of the frequency associated with the "turbulent energy producing" subrange maximum at the low frequency end of the -5/3 slope (inertial subrange) region.

2 Gap is the inverse of the frequency where a minimum occurs on the low frequency side of the "turbulent energy producing" subrange.

3 Slope is the log (power) vs. log (frequency) relationship in only the "low frequency" part of the spectrum. Gap frequencies are not included.

Table 5. Summary of wind direction spectra for NPS data depicted in figures 9b, 11b, 13b, 15b, 17b, 19b, and 21b.

DATE	RANGE(km)	N	MEAN1(m)	STD DEV2(m)	SKEW3	KURTOSIS4	W5
21Jun82	2	25	-293.0	149.7	-0.2861	-0.3701	0.9705
21Jun82	4	26	-356.5	255.6	+0.6759	+0.0095	0.9554
22Jun82	4	43	-1733.7	392.1	-0.0101	-0.6845	0.9721
24Jun82	2	13	-80.5	110.3	+0.8840	+0.6898	0.9077
24Jun82	4	34	-678.0	391.5	-0.4567	+1.0885	0.9590
25Jun82	2	14	-201.3	50.4	+0.7334	-0.8242	0.8912
25Jun82	4	38	-740.9	166.3	+0.7936	+0.8523	0.9474
27Jun82	2	9	-185.9	103.3	-0.0621	-0.0441	0.9567
27Jun82	4	17	-895.4	198.8	-0.1541	-0.1224	0.9674
27Jun82	6	4	-1516.6	415.4	+1.2242	-0.7663	[illegible]
28Jun82	2	6	-417.3	83.4	+0.8019	-0.1838	[illegible]
28Jun82	4	12	-795.0	260.9	-0.1653	+1.4008	[illegible]
28Jun82	6	6	-970.6	160.5	-1.3268	+1.7325	[illegible]
28Jun82	8	5	-1165.7	467.0	+2.1248	+4.6043	[illegible]
29Jun82	2	3	-613.9	477.9	+0.9695	-------	[illegible]
29Jun82	4	12	-913.0	1008.9	+0.6763	+0.0379	[illegible]
29Jun82	6	9	-789.9	966.7	+0.8435	-1.0370	[illegible]
29Jun82	8	11	-1177.6	1380.2	+1.2122	+0.7888	[illegible]

1 MEAN: Mean position of plume center (as measured from the mean wind centerline) of mass distribution for a given range bin.

2 STD DEV: Standard deviation of plume center of mass for a given range bin.

3 SKEWNESS: Measures the tendency of deviations to be larger in one direction than the other. Values are unbounded. Positive values indicate a "tail" of values exists in the values larger than the mean, negative values indicate a "tail" in smaller values.

4 KURTOSIS: Measures the heaviness of the distribution "tails" (-2.0 < Kurtosis < ∞). Relatively large values indicate normality assumption should be questioned, but this statistic is unstable for a small number of samples which is characteristic of this experiment.

5 W: Shapiro-Wilk statistic for the center of mass distribution. Measures the normality of the distribution (0.0 < W < 1.0). Values close to 1.0 indicate more normal distributions.

Table 6. Meander statistics for NPS meander data . N is the number of profiles for a given crosswind center of mass distribution.

While we were not able to parameterize meander with mean surface layer meteorological variables, direct measurements of lateral turbulence intensity did correlate well with the observed meander standard deviations. Taylor (1921) predicts that when the length scale of turbulence is much larger than the scale of the plume (sigma-y meander in this case) the following simple formula will apply:

$$\sigma_{ym} = i_v x \tag{5}$$

where σ_{ym} is the single-particle lateral standard deviation, or sigma-y meander,

i_v is the lateral turbulence intensity,

x is downwind distance.

This is often referred to as the "near-field" approximation to single-particle diffusion. For application to the present analysis, we define the lateral turbulence intensity as

$$i_v = \frac{\langle v^2 \rangle^{1/2}}{U} \tag{6}$$

where $\langle v^2 \rangle$ is the variance of the crosswind component measured over the travel time of the tracer (approximately 1/2 hour) and averaged over the entire day.

U is the mean wind speed

Figures 22-28 show equation (5) plotted for each experimental day with the standard deviations of table 5 (sigma-y meander) depicted as data points. Also shown is a least-squared linear fit to the data.

Note the good agreement between this simple model and the observed data in almost every case. The key to success is matching the travel time of the plume to the RMS window in the turbulence intensity measurement. Also, since the measured variance is highly non-stationary, it is necessary to average this quantity over a full day.

The agreement between the data and the near-field approximation is also supported by our spectral results. The spectra continue to increase in power through the entire spectral window (4-8 hr^{-1}) which suggests that turbulent motions operating at these very low frequencies have very long time scales as equation (5) assumes.

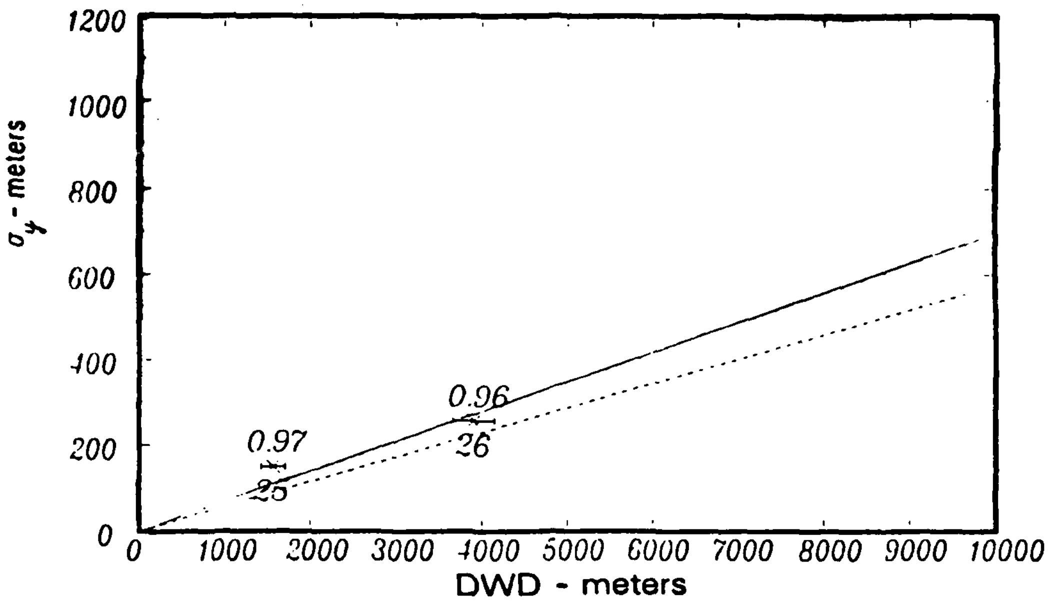

Figure 22. Sigma-y meander vs. downwind distance. Error bars are the standard deviations of downwind distance positions for a given range bin. Upper number is Shapiro-Wilk statistic and lower is number of data points. Solid line is best fit to data. Dashed line is equation 5. Data is NPS, 21 June 1982.

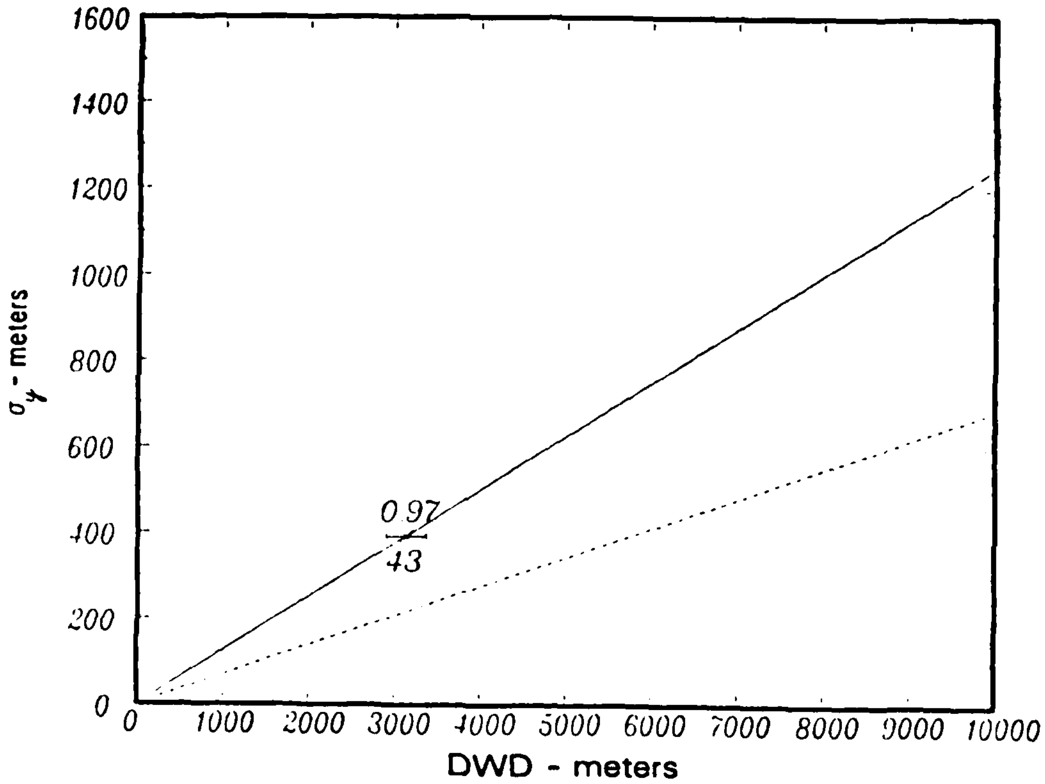

Figure 23. Same as figure 22, except NPS data, 22 June 1982.

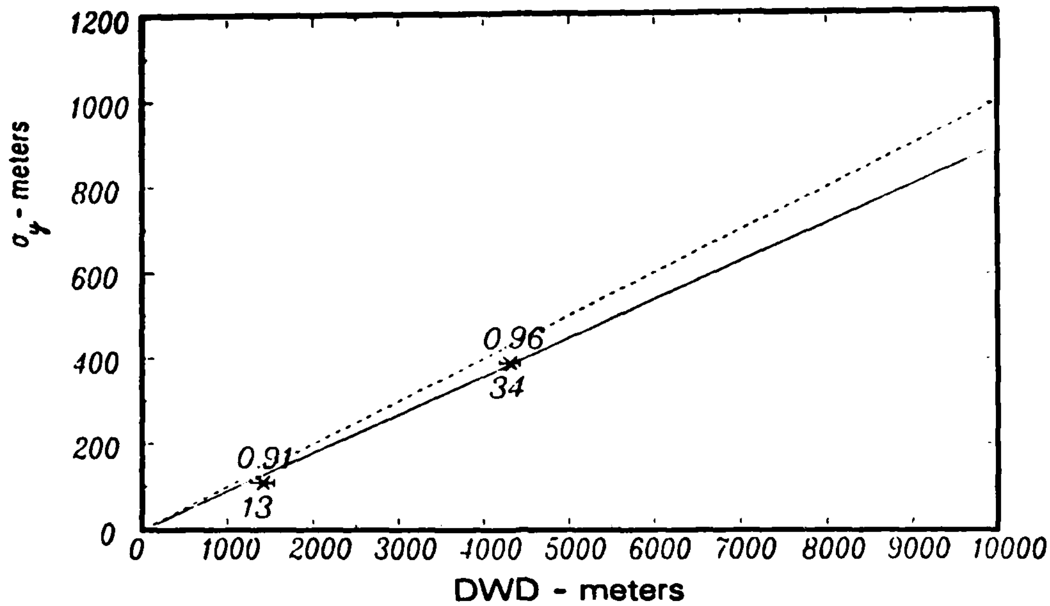

Figure 24. Same as figure 22, except NPS data, 24 June 1982.

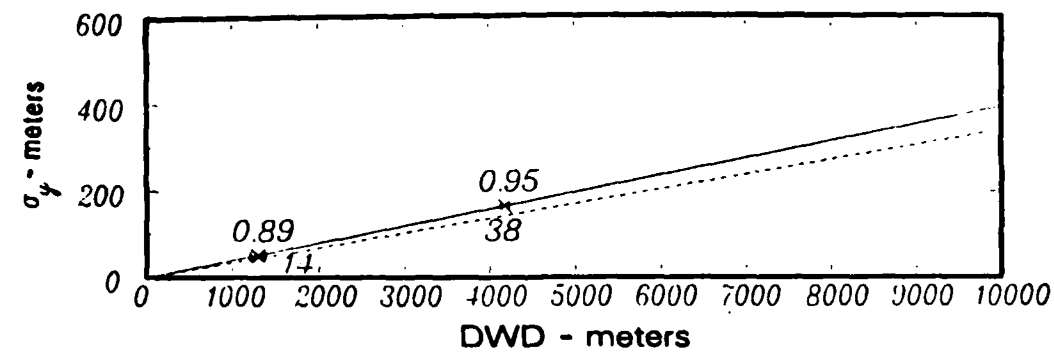

Figure 25. Same as figure 22, except NPS data, 25 June 1982.

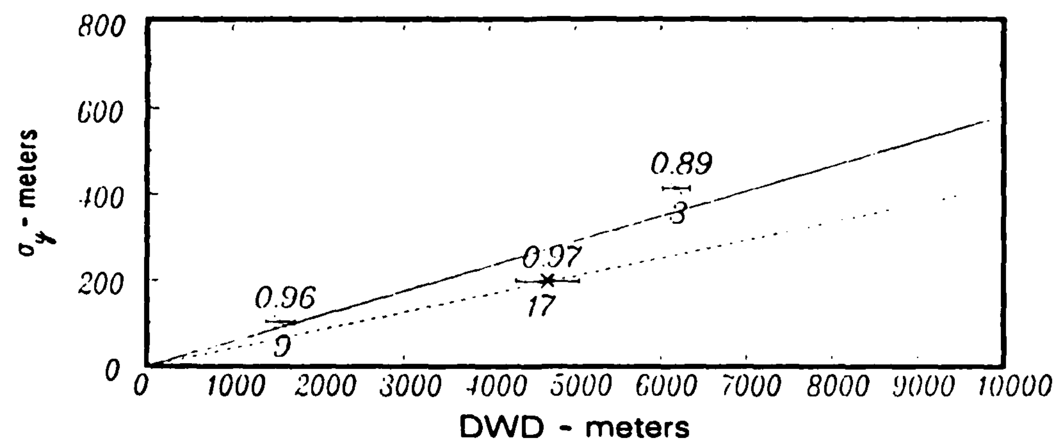

Figure 26. Same as figure 22, except NPS data, 27 June 1982.

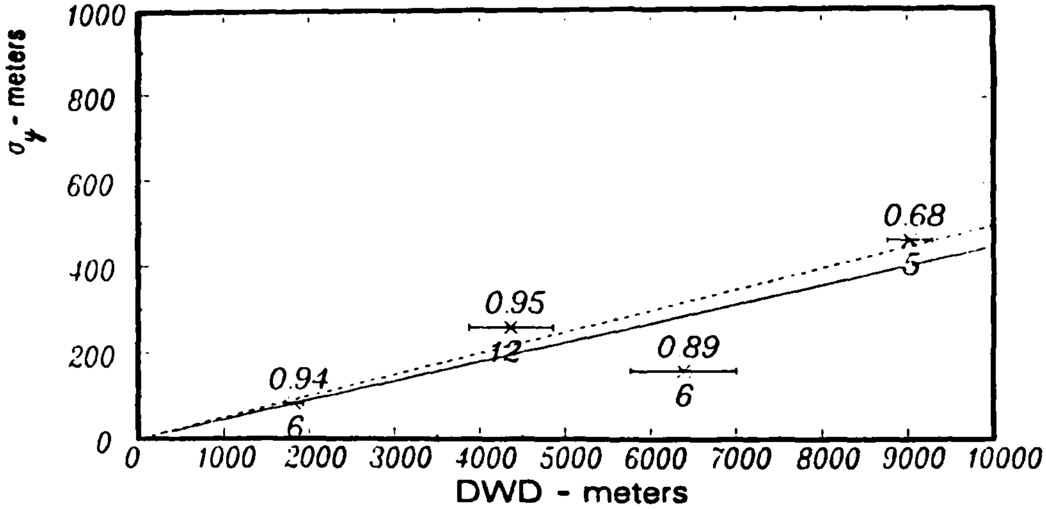

Figure 27. Same as figure 22, except NPS data, 28 June 1982.

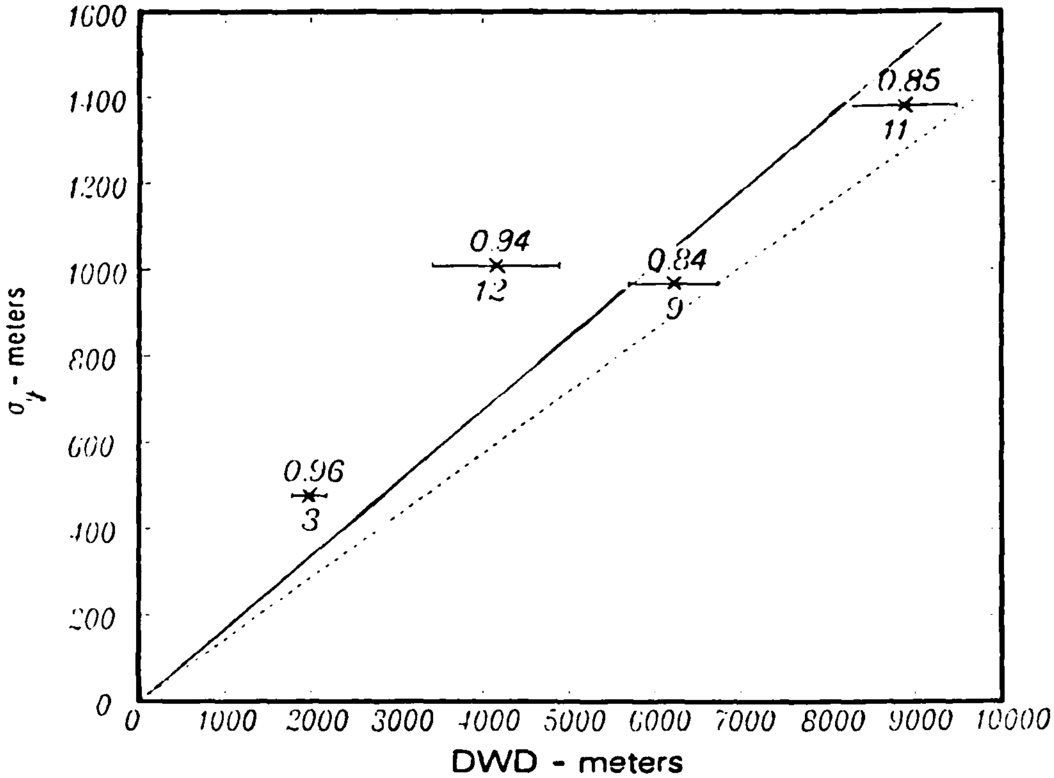

Figure 28. Same as figure 22, except NPS data, 29 June 1982.

5. CHEMICAL WEAPONS HAZARD FORECAST PROGRAM MODIFICATIONS

Part of the current research work is to modify the Chemical Weapons Hazard Forecast Program (CWHFP). This section assumes the reader is familiar with that program and understands the program's design, inputs, and operation. EPG modified the 24 May 1984 "test and evaluation" version of this program supplied to EPG by J. Branum (1984). Later versions of this model may exist, and the following modifications can be easily transplanted into such hybrids.

The proposed modifications specifically make use of the parameterizations described above and are designed so as to supply the user with a better understanding of the character of atmospheric diffusion processes, and hopefully, more information on how to avoid hazards. The previous model used meteorological inputs to calculate a stability category, and then calculate one hour averaged plume dimensions based on stability dependent sigma-y and sigma-z algorithms. This version uses the same stability scheme, but replaces the one-hour sigma-y functions with the relative diffusion parameterization presented above. Sigma-z parameterizations are unchanged. The resultant isopleths represent either "dosage" values from an instantaneous "burst" release or a concentration "snapshot" from a continuous plume.

In order to present the meander of a plume (offaxis excursions of a puff) the single-particle parameterization developed above is used to obtain a "meander envelope." This envelope is simply the 2 sigma-y position of the plume or puff center of mass distribution representing a 95% probability of impact. This envelope is superimposed on the instantaneous isopleths in order to show the combined impact of the two diffusion processes. An artificial "ripple" is convolved into the instantaneous solution to offer the user a visualization of meander. The frequency and amplitude of this ripple has no physical basis, and is only installed to help the user understand the nature of the meander process.

Figures 29-36 show several examples of model output. Labels display lethal dose levels on the instantaneous isopleths and a footnote explains the meander envelope. Instruction manuals should explain the arbitrary nature of the ripple in order to avoid false conclusions based on these plots. Note the change in the frequency of the ripple as the meander envelope shrinks (see figures 29, 30, 31 or 32, 33, 34). This change again was arbitrary , and was only intended to suggest the possibility that the important eddy sizes decrease as the meander decreases. The amplitude of the ripple, again, was arbitrary (selected to be 1 sigma-y meander) and suggests that the instantaneous position of the cloud is somewhat random and rarely reaches the meander envelope bounds. Also note the change in the instantaneous cloud dimensions with a change in stability class (figures 29, 30, 31,

CHEMICAL WEAPON HAZARD FORECAST PROGRAM - SNAP XX.X

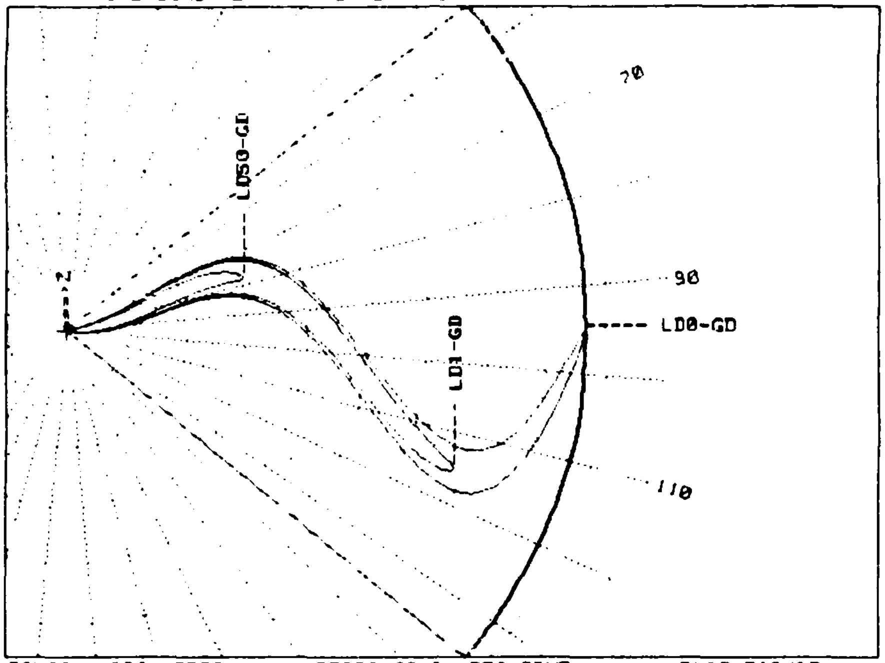

RINGS = 300 YARDS BEARINGS IN DEG TRUE PLOT FORMAT #1

TERRAIN TYPE	OPEN-SEA	
MEAN WIND	10 KTS	FROM 275 DEG TRUE
SIGMA WIND DIRECTION	20 DEG	
MEAN AIR TEMP	10 DEG C	
MEAN SEA-SURFACE TEMP	17 DEG C	
RELATIVE HUMIDITY	70 %	
SURFACE MIXING LAYER HT	0 METERS BASED ON ** DEFAULT **	
STABILITY CATAGORY	B MODIFIED PASQUILL	
MUNITION TYPE	MK116-SIZE BOMB/MISSILE	
SOURCE TYPE	POINT-BURST	
SOURCE SIZE (effective)	88 KG	
SOURCE RATE	INSTANTANEOUS	

****

CONTOUR LABEL (DOSE-AGENT)	POTENTIAL CASUALTY EFFECTS (WITHOUT PROTECTION)	APPROX MAX RANGE
- LD50-GD	50% DEATHS - MOST INCAPACITATED	875 YARDS
- LD1-GD	1% DEATHS - MANY INCAPACITATED	1933 YARDS
- LD0-GD	NO DEATHS - SOME INCAPACITATED	2588 YARDS

OUTSIDE (THICK) CONTOUR IS 95% PROBABILITY THAT CENTER OF MASS WILL CROSS

Figure 29. Chemical Weapons Hazard Forecast Program output sample -- unstable atmosphere, large meander.

CHEMICAL WEAPON HAZARD FORECAST PROGRAM - SNAP XX.X

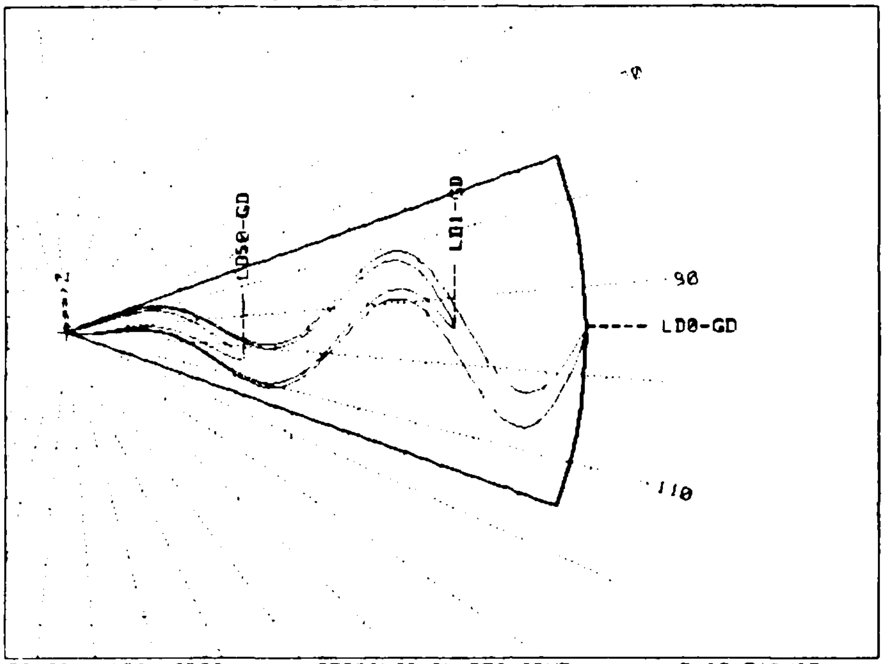

RINGS = 300 YARDS   BEARINGS IN DEG TRUE   PLOT FORMAT #1

TERRAIN TYPE	OPEN-SEA		
MEAN WIND	10	KTS	FROM 275 DEG TRUE
SIGMA WIND DIRECTION	10	DEG	
MEAN AIR TEMP	10	DEG C	
MEAN SEA-SURFACE TEMP	17	DEG C	
RELATIVE HUMIDITY	70	%	
SURFACE MIXING LAYER HT	0	METERS BASED ON ** DEFAULT **	
STABILITY CATAGORY	B	MODIFIED PASQUILL	
MUNITION TYPE	MK116-SIZE BOMB/MISSILE		
SOURCE TYPE	POINT-BURST		
SOURCE SIZE (effective)	88	KG	
SOURCE RATE	INSTANTANEOUS		

CONTOUR LABEL (DOSE-AGENT)	POTENTIAL CASUALTY EFFECTS (WITHOUT PROTECTION)	APPROX MAX RANGE
- LD50-GD	50% DEATHS - MOST INCAPACITATED	875 YARDS
- LD1-GD	1% DEATHS - MANY INCAPACITATED	1933 YARDS
- LD0-GD	NO DEATHS - SOME INCAPACITATED	2588 YARDS

OUTSIDE (THICK) CONTOUR IS 95% PROBABILITY THAT CENTER OF MASS WILL CROSS

Figure 30. Chemical Weapons Hazard Forecast Program output sample -- unstable atmosphere, moderate meander.

CHEMICAL WEAPON HAZARD FORECAST PROGRAM - SNAP XX.X

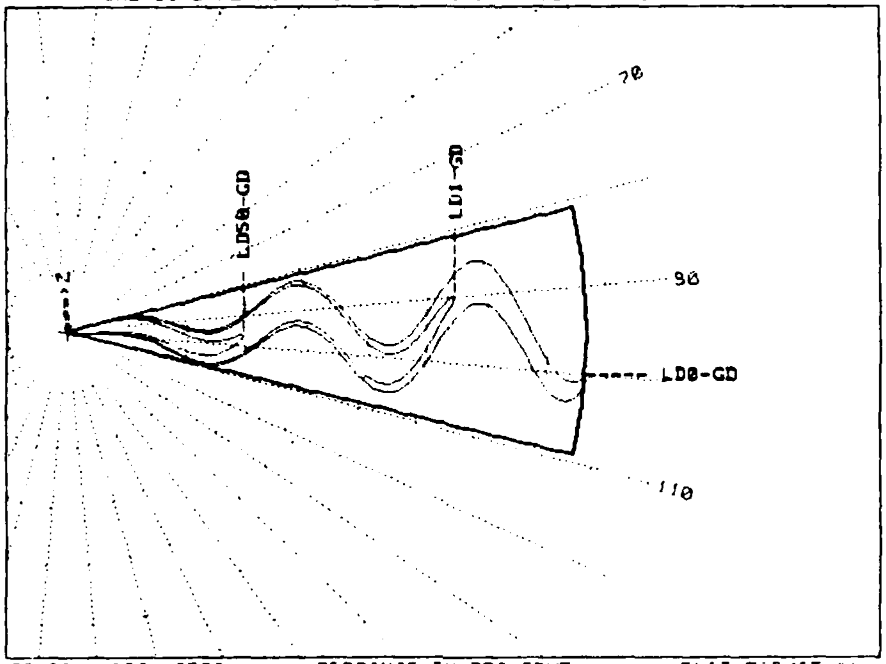

RINGS = 300 YARDS   BEARINGS IN DEG TRUE   PLOT FORMAT #1

TERRAIN TYPE	OPEN-SEA	
MEAN WIND	10 KTS	FROM 275 DEG TRUE
SIGMA WIND DIRECTION	7 DEG	
MEAN AIR TEMP	10 DEG C	
MEAN SEA-SURFACE TEMP	17 DEG C	
RELATIVE HUMIDITY	70 %	
SURFACE MIXING LAYER HT	0 METERS BASED ON ** DEFAULT **	
STABILITY CATAGORY	B MODIFIED PASQUILL	
MUNITION TYPE	MK116-SIZE BOMB/MISSILE	
SOURCE TYPE	POINT-BURST	
SOURCE SIZE (effective)	80 KG	
SOURCE RATE	INSTANTANEOUS	

****

CONTOUR LABEL (DOSE-AGENT)	POTENTIAL CASUALTY EFFECTS (WITHOUT PROTECTION)	APPROX MAX RANGE
- LD50-GD	50% DEATHS - MOST INCAPACITATED	875 YARDS
- LD1-GD	1% DEATHS - MANY INCAPACITATED	1933 YARDS
- LD0-GD	NO DEATHS - SOME INCAPACITATED	2580 YARDS

OUTSIDE (THICK) CONTOUR IS 95% PROBABILITY THAT CENTER OF MASS WILL CROSS

Figure 31. Chemical Weapons Hazard Forecast Program output sample -- unstable atmosphere, small meander.

CHEMICAL WEAPON HAZARD FORECAST PROGRAM - SNAP XX.Y

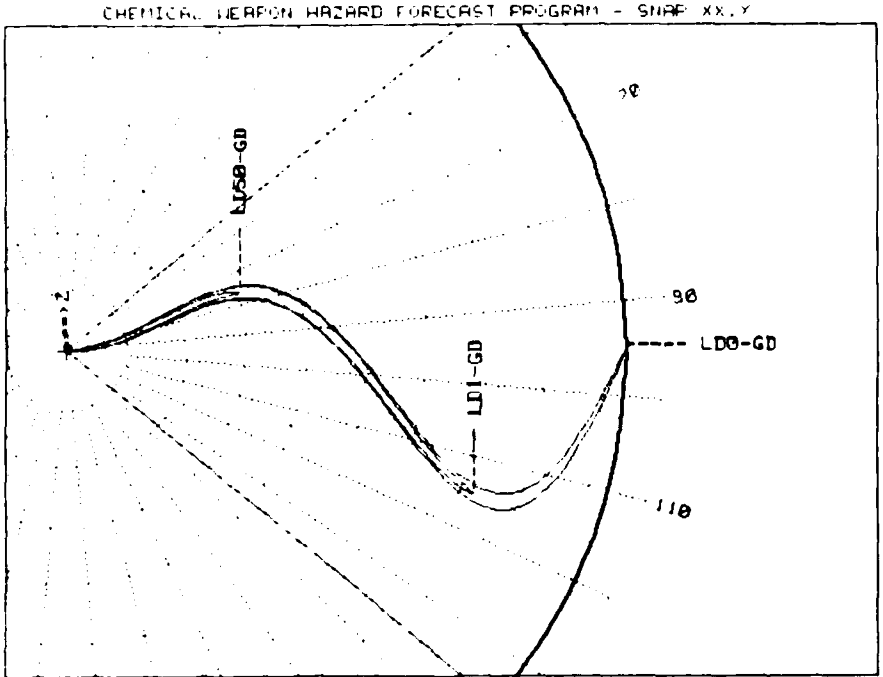

RINGS = 2000 YARDS BEARINGS IN DEG TRUE PLOT FORMAT #1

TERRAIN TYPE	OPEN-SEA		
MEAN WIND	10	KTS	FROM 275 DEG TRUE
SIGMA WIND DIRECTION	20	DEG	
MEAN AIR TEMP	17	DEG C	
MEAN SEA-SURFACE TEMP	10	DEG C	
RELATIVE HUMIDITY	70	%	
SURFACE MIXING LAYER HT	0	METERS BASED ON ** DEFAULT **	
STABILITY CATAGORY	E	MODIFIED PASQUILL	
MUNITION TYPE	MK116-SIZE BOMB/MISSILE		
SOURCE TYPE	POINT-BURST		
SOURCE SIZE (effective)	88	KG	
SOURCE RATE	INSTANTANEOUS		

CONTOUR LABEL (DOSE-AGENT)	POTENTIAL CASUALTY EFFECTS (WITHOUT PROTECTION)	APPROX MAX RANGE
- LD50-GD	50% DEATHS - MOST INCAPACITATED	5776 YARDS
- LD1-GD	1% DEATHS - MANY INCAPACITATED	13597 YARDS
- LD0-GD	NO DEATHS - SOME INCAPACITATED	18636 YARDS

OUTSIDE (THICK) CONTOUR IS 95% PROBABILITY THAT CENTER OF MASS WILL CROSS

Figure 32. Chemical Weapons Hazard Forecast Program output sample -- stable atmosphere, large meander.

CHEMICAL WEAPON HAZARD FORECAST PROGRAM - SNAP XX.X

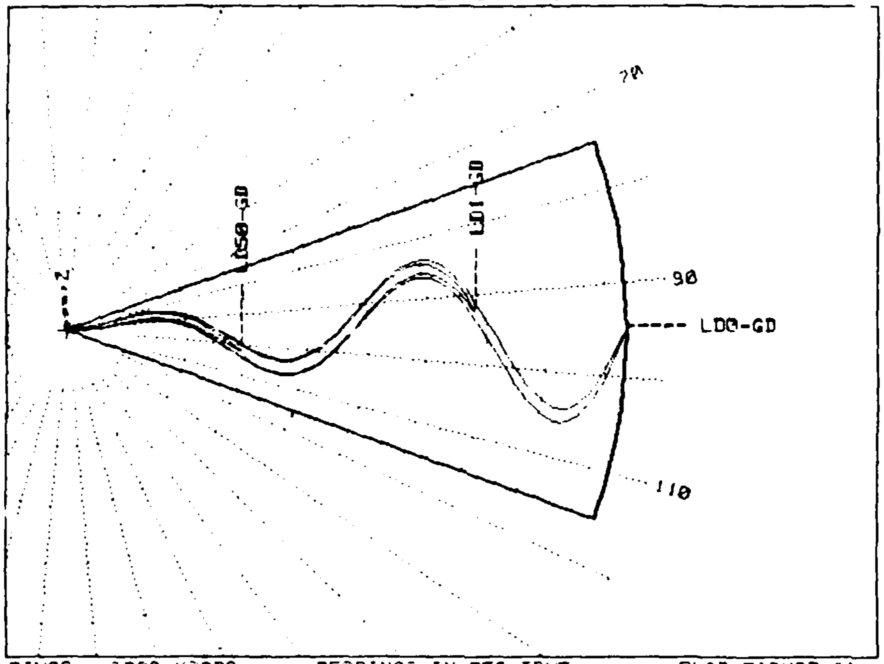

RINGS = 2000 YARDS BEARINGS IN DEG TRUE PLOT FORMAT #1

TERRAIN TYPE	OPEN-SEA	
MEAN WIND	10 KTS	FROM 275 DEG TRUE
SIGMA WIND DIRECTION	10 DEG	
MEAN AIR TEMP	17 DEG C	
MEAN SEA-SURFACE TEMP	10 DEG C	
RELATIVE HUMIDITY	70 %	
SURFACE MIXING LAYER HT	0 METERS BASED ON ** DEFAULT **	
STABILITY CATAGORY	E MODIFIED PASQUILL	
MUNITION TYPE	MK116-SIZE BOMB-MISSILE	
SOURCE TYPE	POINT-BURST	
SOURCE SIZE (effective)	80 KG	
SOURCE RATE	INSTANTANEOUS	

****

CONTOUR LABEL (DOSE-AGENT)	POTENTIAL CASUALTY EFFECTS (WITHOUT PROTECTION)	APPROX MAX RANGE
- LD50-GD	50% DEATHS - MOST INCAPACITATED	5778 YARDS
- LD1-GD	1% DEATHS - MANY INCAPACITATED	13597 YARDS
- LD0-GD	NO DEATHS - SOME INCAPACITATED	18638 YARDS

OUTSIDE (THICK) CONTOUR IS 95% PROBABILITY THAT CENTER OF MASS WILL CROSS

Figure 33. Chemical Weapons Hazard Forecast Program output sample -- stable atmosphere, moderate meander.

CHEMICAL WEAPON HAZARD FORECAST PROGRAM - SNAP ...

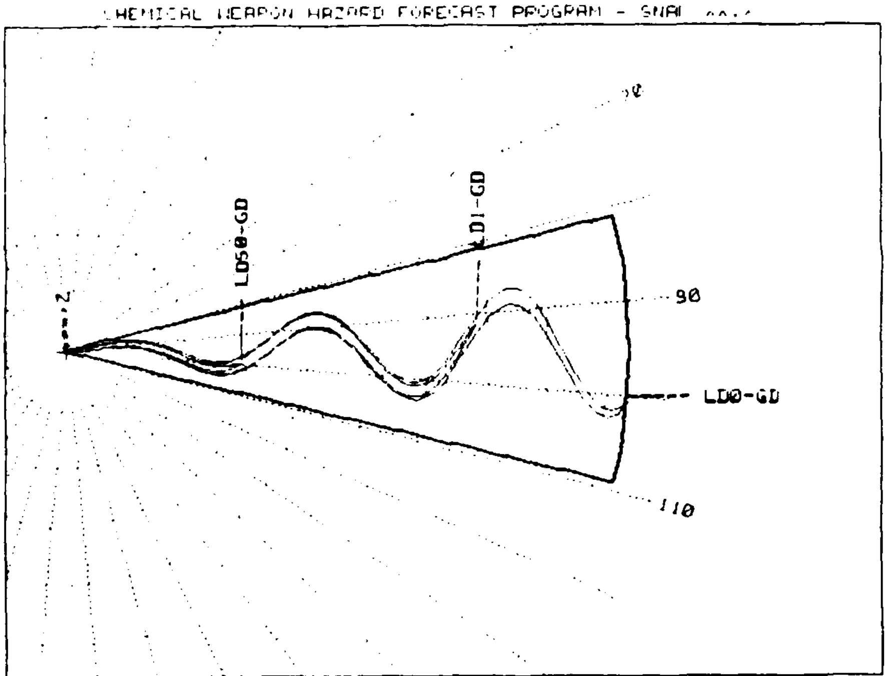

RINGS = 2000 YARDS   BEARINGS IN DEG TRUE   PLOT FORMAT #1

TERRAIN TYPE	OPEN-SEA	
MEAN WIND	10 KTS	FROM 275 DEG TRUE
SIGMA WIND DIRECTION	7 DEG	
MEAN AIR TEMP	17 DEG C	
MEAN SEA-SURFACE TEMP	10 DEG C	
RELATIVE HUMIDITY	70 %	
SURFACE MIXING LAYER HT	0 METERS BASED ON ** DEFAULT **	
STABILITY CATAGORY	E MODIFIED PASQUILL	
MUNITION TYPE	MK116-SIZE BOMB MISSILE	
SOURCE TYPE	POINT-BURST	
SOURCE SIZE (effective)	88 KG	
SOURCE RATE	INSTANTANEOUS	

****

CONTOUR LABEL (DOSE-AGENT)	POTENTIAL CASUALTY EFFECTS (WITHOUT PROTECTION)	APPROX MAX RANGE
- LD50-GD	50% DEATHS - MOST INCAPACITATED	5778 YARDS
- LD1-GD	1% DEATHS - MANY INCAPACITATED	13597 YARDS
- LD0-GD	NO DEATHS - SOME INCAPACITATED	18638 YARDS

OUTSIDE (THICK) CONTOUR IS 95% PROBABILITY THAT CENTER OF MASS WILL CROSS

Figure 34. Chemical Weapons Hazard Forecast Program output sample -- stable atmosphere, small meander.

CHEMICAL WEAPON HAZARD FORECAST PROGRAM - SNAP XX.X

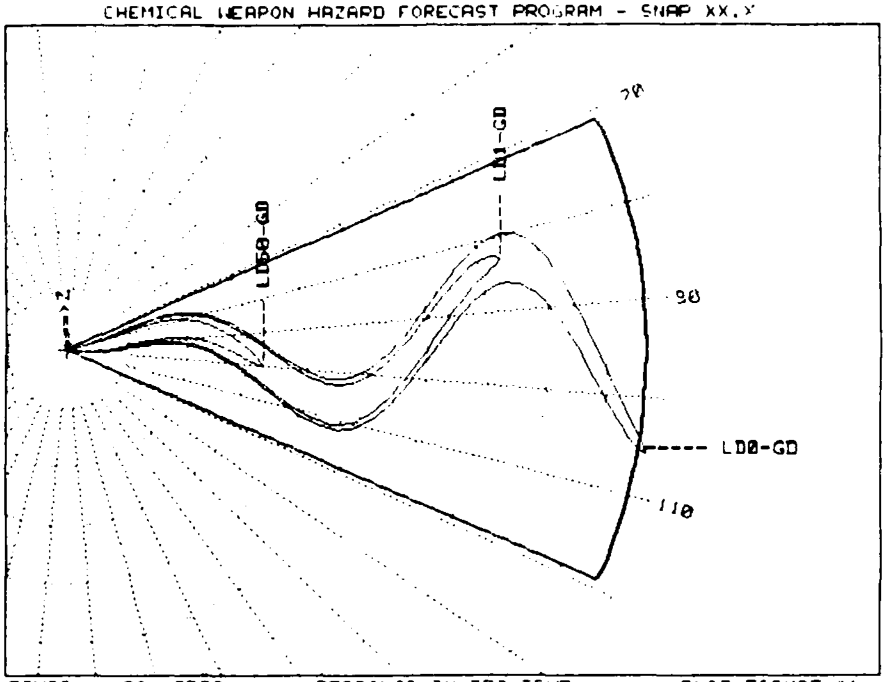

RINGS = 400 YARDS BEARINGS IN DEG TRUE PLOT FORMAT #1

TERRAIN TYPE	OPEN-SEA
MEAN WIND	5 KTS FROM 275 DEG TRUE
SIGMA WIND DIRECTION	12 DEG
MEAN AIR TEMP	10 DEG C
MEAN SEA-SURFACE TEMP	17 DEG C
RELATIVE HUMIDITY	70 %
SURFACE MIXING LAYER HT	0 METERS BASED ON ** DEFAULT **
STABILITY CATAGORY	B MODIFIED PASQUILL
MUNITION TYPE	MK116-SIZE BOMB/MISSILE
SOURCE TYPE	POINT-BURST
SOURCE SIZE (effective)	88 KG
SOURCE RATE	INSTANTANEOUS

****

CONTOUR LABEL (DOSE-AGENT)	POTENTIAL CASUALTY EFFECTS (WITHOUT PROTECTION)	APPROX MAX RANGE
- LD50-GD	50% DEATHS - MOST INCAPACITATED	1301 YARDS
- LD1-GD	1% DEATHS - MANY INCAPACITATED	2872 YARDS
- LD0-GD	NO DEATHS - SOME INCAPACITATED	3846 YARDS

OUTSIDE (THICK) CONTOUR IS 95% PROBABILITY THAT CENTER OF MASS WILL CROSS

Figure 35. Chemical Weapons Hazard Forecast Program output sample -- light wind conditions.

CHEMICAL WEAPON HAZARD FORECAST PROGRAM - SNAP xx.x

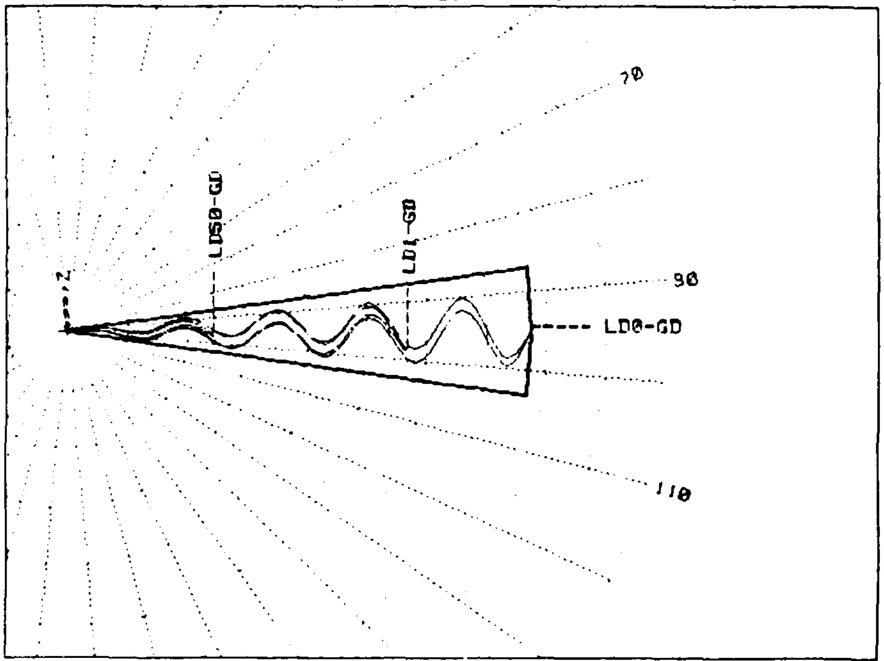

RINGS = 1000 YARDS   BEARINGS IN DEG TRUE   PLOT FORMAT #1

TERRAIN TYPE	OPEN-SEA		
MEAN WIND	20	KTS	FROM 275 DEG TRUE
SIGMA WIND DIRECTION	4	DEG	
MEAN AIR TEMP	17	DEG C	
MEAN SEA-SURFACE TEMP	10	DEG C	
RELATIVE HUMIDITY	70	%	
SURFACE MIXING LAYER HT	0	METERS BASED ON ** DEFAULT **	
STABILITY CATAGORY	D	MODIFIED PASQUILL	
MUNITION TYPE	MK116-SIZE BOMB/MISSILE		
SOURCE TYPE	POINT-BURST		
SOURCE SIZE (effective)	86	KG	
SOURCE RATE	INSTANTANEOUS		

CONTOUR LABEL (DOSE-AGENT)	POTENTIAL CASUALTY EFFECTS (WITHOUT PROTECTION)	APPROX MAX RANGE
- LD50-GD	50% DEATHS - MOST INCAPACITATED	2443 YARDS
- LD1-GD	1% DEATHS - MANY INCAPACITATED	5660 YARDS
- LD0-GD	NO DEATHS - SOME INCAPACITATED	7714 YARDS

OUTSIDE (THICK) CONTOUR IS 95% PROBABILITY THAT CENTER OF MASS WILL CROSS

Figure 36. Chemical Weapons Hazard Forecast Program output sample -- strong wind conditions.

vs. 32, 33, 34) or wind speed (figures 35 vs. 36) as would be qualitatively predicted by a Gaussian model. This model requires one additional user input over those needed in the previous version; the standard deviation of the wind direction used in the meander calculations. As stated in the previous sections, the averaging time must be the cloud travel time to the distance of interest. Also, the value used should be the average of several such standard deviations obtained over a significant fraction of the day. The sampling time is not critical , 1.0 - 0.1 Hz would be sufficient.

Code modifications are listed in figures 37-40. Figure 37 shows both the turbulence intensity input and the revised sigma parameter table (relative diffusion). Figure 38 shows where the meander envelope is calculated while figures 39-40 list the plotting routine.

a)

```
420   !
430   Mean_wind_sp_kt=5      ! KTS
440   Mean_wind_dir=275      ! DEG TRUE
450   !
460   Mix_layer_ht=0         ! METERS
470   !
480   ! $$$$$ NEW 1985 $$$$$$$$$
490   Turb_intens=12*PI/180    ! turbulence intensity (radians) input
500   ! $$$$$$$$$$$$$$$$$$$$$$$$$
510   !
520   DIM Ml_ht_est_meth$[30]
530   Ml_ht_est_meth$="** DEFAULT **"
540   !
```

b)

```
3790  ! LOAD ARRAY CONTAINING VALUES OF Ap->Dp
3800  !
3810  FOR P0=1 TO 6  ! WHERE P0 = NUMERICAL REFERENCE TO STABILITY CLASSES
3820  !                (1="A" -> 6="F")
3830    READ Matrix_ap(P0),Matrix_bp(P0),Matrix_cp(P0),Matrix_dp(P0)
3840  NEXT P0
3850  !
3860  ! $$$$$$$ NEW 1985 $$$$$$$$$
3870  !
3880  DATA 0,0,0,0                ! -- CAT "A" (NOT USED OVER THE OCEAN)
3890  DATA 0.0410,1.00,0.32,0.75 ! -- CAT "B"
3900  DATA 0.0410,1.00,0.32,0.70 ! -- CAT "C"  sigmas are for relative diffusion
3910  DATA 0.0211,1.00,0.16,0.65 ! -- CAT "D"  in lateral direction only
3920  DATA 0.0211,1.00,0.10,0.62 ! -- CAT "E"
3930  DATA 0,0,0,0                ! -- CAT "F->"(NOT DEFINED OR USED BY THIS MODEL)
3940  !
3950  ! $$$$$$$$$$$$$$$$$$$$$$$$$$$
3960  !
```

Figure 37. Abbreviated listing of CWHFP showing (a) turbulence intensity input and (b) new array of sigma parameters.

```
5710 ! **********************************************************************
5720  !
5730 Pt_vapor_nomix:! CALC MODEL FOR POINT SOURCES OF GASEOUS AGENTS,
5740  !                AND NO REFLECTIVE MIXING LAYER CAP
5750  !
5760  !
5770  !
5780  !  $$$$$ NEW 1985 $$$$
5790  DIM Meand_x(100),Meand_y(100)
5800 DIM Data_set_x(3,100),Data_set_y(3,100)  ! 100 points vs. 20 pts
5810 Points_per_set=100 !                        in old version
5820  ! $$$$$$$$$$$$$$$$$$$$
5830 !
5840  M_to_yds=39.37/36    ! CONVERSION FACTOR USED IN EQUATIONS BELOW, DEFINED
5850  !                      AGAIN HERE TO PERMIT TESTING OF PARTIAL PROGRAM
5860  !
5870  FOR K=1 TO Num_data_sets
5880 Partial_1(K)=Source_size(K)/(PI*60*Mean_wind_sp_m*Dose_val(K))
5890 Max_range_x(K)=(Partial_1(K)/(Ap(K)*Cp(K)))^(1/(Bp(K)+Dp(K)))
5900 Data_set_y(K,0)=0
5910  X_increment=Max_range_x(K)/Points_per_set
5920  IF X_increment=0 THEN X_increment=1  ! ADDED TO PREVENT BLOWUP ON BAD DATA
5930  !
5940 FOR J=1 TO Points_per_set
5950 X=J*X_increment
5960 Data_set_x(K,J)=X
5970 Sigma_yx=Ap(K)*X^Bp(K)   ! ASSUMES NO INITIAL CLOUD SIZE FOR CONSERVATISM
5980 Sigma_zx=Cp(K)*X^Dp(K)
5990 Partial_2(K)=2*LOG(Partial_1(K)/(Sigma_yx*Sigma_zx))
6000 IF Partial_2(K)<0 THEN Partial_2(K)=0 ! PREVENT POSSIBLE ERROR IN LATER SQR
                                             CALCULATIONS
6010 Data_set_y(K,J)=Sigma_yx*SQR(Partial_2(K))
6020 NEXT J
6030 NEXT K
6040  !
6050  ! $$$$$ NEW 1985 $$$$$$$$$
6060  RAD
6070  FOR J=1 TO Points_per_set
6080  X=J*X_increment
6090  IF X>Max_range_x(Num_data_sets)*COS(2*Turb_intens) THEN GOTO Close
6100  Meand_y(J)=X*TAN(2*Turb_intens)     ! meander envelope is based
6110  Meand_x(J)=X !                    only  on turbulence intensity and
6120  GOTO J100 !                  selected to be the 2 sigma value (95%)
6130  !
6140 Close: Meand_y(J)=SQR(Max_range_x(Num_data_sets)^2-X^2) ! stop envelope
6150        Meand_x(J)=X !   at maximum range and close with partial circle
6160 J100: NEXT J
6170  MAT Meand_x=Meand_x*(M_to_yds)
6180  MAT Meand_y=Meand_y*(M_to_yds)
6190  !
6200  ! $$$$$$$$$$$$$$$$$$$$$$$$
```

Figure 38. Abbreviated listing of CWHFP showing calculation of the meander envelope. Points per data set may be adjusted for speed or better resolution.

```
8190  ! $$$$$ NEW 1985 $$$$$$$$$$$$
8200  DIM Scaled_x(100),Scaled_y(100)    ! LIMITS BASED ON "POINTS_PER_SET"
8210  DIM Contour_labl_x(3),Contour_labl_y(3)  ! LIMIT BASED ON NUM_DATA_SETS
8220  !
8230  FOR Point_num=0 TO Points_per_set    ! POINTS_PER_SET preset above
8240  Scaled_x(Point_num)=Meand_x(Point_num)*Scale_factor ! scale meander
8250  Scaled_y(Point_num)=Meand_y(Point_num)*Scale_factor ! envelope
8260  NEXT Point_num
8270  GOSUB Plot_meander
8280  !
8290  ! $$$$$$$$$$$$$$$$$$$$$$$$$$
8300  !
8310  FOR Set_num=1 TO Num_data_sets       ! NUM_DATA_SETS PRESET TO "3", ABOVE
8320  !
8330  FOR Point_num=0 TO Points_per_set    ! POINTS_PER_SET PRESET  ABOVE
8340  Scaled_x(Point_num)=Data_set_x(Set_num,Point_num)*Scale_factor
8350  Scaled_y(Point_num)=Data_set_y(Set_num,Point_num)*Scale_factor
8360  NEXT Point_num
8370  GOSUB Plot_contour
8380  Contour_labl_x(Set_num)=Scaled_x(Points_per_set)
8390  !
8400  ! $$$$$$$$$ NEW 1985 $$$$$$$$$$$$$$$$$$$$$$$$$$$$
8410  RAD
8420  R=Data_set_x(Set_num,Points_per_set)/Data_set_x(Num_data_sets,Points_per_s
et) ! dimensionless distance from source [0,1]
8430  Omega=40*PI/180/Turb_intens ! ARBITRARY frequency of ripple oscillation
8440  A=Scaled_x(Points_per_set)*TAN(Turb_intens) ! ARBITRARY ripple amplitude
8450  Ripple=A*SIN(Omega*PI*R) ! offset for y position
8460  Contour_labl_y(Set_num)=Scaled_y(Points_per_set)+Ripple ! add offset to la
bel position
8470  DEG
8480  ! $$$$$$$$$$$$$$$$$$$$$$$$$$$$$$$$$$$$$$$$$$$$$$$
8490  !
8500  NEXT Set_num
8510  GOTO Exit_data_plot
8520  !
8530  ! $$$$$$$ NEW 1985 $$$$$$$$$$$$$$$$$$$$$$$$$$$$$$  (NEW SUBROUTINE)
8540  !
8550 Plot_meander:   ! SUB to plot meander envelope
8560  LINE TYPE 1
8570 Max_overstrike=1 ! same as "old" version
8580  X_offset=0
8590  ! TOP HALF........................
8600 FOR Strikecount=0 TO Max_overstrike
8610 Y_offset=.33*Strikecount
8620 X_offset=.33*Strikecount ! strikecounts thicken line
8630 MOVE Scaled_x(0),Scaled_y(0)
8640 FOR K=0 TO Points_per_set
8650 DRAW Scaled_x(K)+X_offset,Scaled_y(K)+Y_offset
8660 NEXT K
8670  !                         SCALED_X,Y now contain meander envelope
8680 ! PLOT "BOTTOM" HALF
8690 MOVE Scaled_x(0),Scaled_y(0)
8700 FOR K=0 TO Points_per_set
8710 DRAW Scaled_x(K)+X_offset,-(Scaled_y(K)+Y_offset)
8720 NEXT K
8730  NEXT Strikecount
8740 RETURN
8750  ! $$$$$$$$$$$$$$$$$$$$$$$$$$$
```

Figure 39. Abbreviated listing of CWHFP showing meander envelope plotting routine and contour label locating scheme.

```
8770  ! $$$$$$$ NEW 1985 $$$$$$$$$$$ (REVISED SUBROUTINE)
8780 Plot_contour:  !  plot contours of the scaled data
8790  RAD
8800 LINE TYPE 1
8810  Omega=40*PI/180/Turb_intens ! ARBITRARY frequency of ripple oscillation
8820 !
8830 ! PLOT BEGINNING WITH "TOP" HALF OF CONTOUR
8840 !  ( OVERSTRIKE STUFF OMITTED )
8850 MOVE Scaled_x(0),Scaled_y(0)
8860 FOR K=0 TO Points_per_set
8870  R=Data_set_x(Set_num,K)/Data_set_x(Num_data_sets,Points_per_set) ! dimensi
onless distance from source
8880  A=Scaled_x(K)*TAN(Turb_intens) ! ARBITRARY amplitude of ripple selected to
 be 1 sigma
8890  Ripple=A*SIN(Omega*PI*R) ! offset in y direction
8900 DRAW Scaled_x(K),Scaled_y(K)+Ripple ! add offset
8910 NEXT K
8920 !
8930 ! PLOT "BOTTOM" HALF   .... most same as "top" half
8940 !
8950 MOVE Scaled_x(0),Scaled_y(0)
8960 FOR K=0 TO Points_per_set
8970  R=Data_set_x(Set_num,K)/Data_set_x(Num_data_sets,Points_per_set)
8980  A=Scaled_x(K)*TAN(Turb_intens)
8990  Ripple=A*SIN(Omega*PI*R)
9000 DRAW Scaled_x(K),-(Scaled_y(K)-Ripple) ! subtract offset
9010 NEXT K
9020 DEG
9030 RETURN  ! END OF GOSUB PLOT_CONTOUR
9040  ! $$$$$$$$$$$$$$$$$$$$$$$$$$$$$$$$$$$$$$
```

Figure 40. Abbreviated listing of CWHFP showing plotting of hazard contours based on relative diffusion parameterization. "Wiggles" are a result of a SIN wave imposed on the Gaussian plume model solution.

6. SUMMARY AND FUTURE WORK

The presented work successfully parameterizes relative lateral diffusion from mean meteorological quantities, verified via two independent overwater tracer data sets. Single-particle diffusion is successfully parameterized only through direct measurements of the lateral turbulence intensity. Once this quantity is known, however, the parameterization is well behaved.

Future work should attempt to correlate this lateral turbulence with large scale synoptic features, mesoscale phenomena, radiosondes profiles, or other more easily measured quantities. The GMGO researchers are presently being petitioned for positioning information on their experiments so that a more thorough verification of the single-particle parameterization can proceed in the future.

The model is presently designed for only medium ranges, but could be extended to greater distances. This extension would make results highly dependent on inversion height. Some prognostic or diagnostic estimate of this quantity could be incorporated into the model. Longer range overwater experiments should be researched for plume paramterizations at these distances.

7. REFERENCES

Branum, J. (1984) Personal communications. Lawrence Livermore National Laboratory, Livermore, California.

Groll, A., aufm Kapme, W., and Weber, H. (1983) Downwind Hazard Distances for Pollutants over Land and Sea. 14th International Technical Meeting on Air Pollution Modelling and its Applications; Denmark, Copenhagen, 27-30 Sep 1983. Edited by C. D. Wispelaere, Plenum Pub. Corp.

Mikkelsen, T., and Eckman, R. M. (1983) Instantaneous Observations of Plume Dispersion in the Surface Layer. 14th International Technical Meeting on Air Pollution Modelling and its Applications; Denmark, Copenhagen, 27-30 Sep 1983. Edited by C. D. Wispelaere, Plenum Pub. Corp., p 549.

Sawford, B. L. (1985) Concentration Statistics for Surface Plumes in the Atmospheric Boundary Layer. 7th Symposium on Turbulence and Diffusion; Boulder, Colorado, 12-15 November 1985. American Meteorological Society, Boston, Massachusetts, p 323.

Schacher, G. E., Spiel, D. E., Fairfall, C. W., Davidson, K. L., Leonard, C. A., and Reheis, C. H. (1982) California Coastal Offshore Transport and Diffusion Experiments - Meteorological Conditions and Data. NPS-61-82-007, Naval Postgraduate School, Monterey, California 93943, 379 pp.

Shapiro, S. S., and Wilk, M. B. (1965) An Analysis of Variance Test for Normality (Complete Samples). Biometrika, 52, 591-611.

Skupniewicz, C. E., and Schacher, G. E. (1984) Measured Plume Dispersion Parameters over Water. NPS-61-84-B12, Naval Postgraduate School, Monterey, California 93943, 101 pp.

Skupniewicz, C. E., and Schacher, G. E. (1984) Assessment of the Performance of an In-field Gaussian Plume/Puff Model of Overwater Use. NPS-61-85-002, Naval Postgraduate School, Monterey, California 93943, 47 pp.

Smith, F. B., and Hay, J. S. (1961) The Expansion of Clusters of Particles in the Atmosphere. Q. J. R. Meteorol. Soc., 87 (371), 82-101.

Taylor, G. I. (1921) Diffusion by Continuous Movements. Proc. London Math. Soc., 20, 196.

Turner, D. B. (1967) Workbook of Atmospheric Dispersion Estimates, Public Health Service, Pub. no. 99-AP-26, Robert A. Taft Sanitary Eng. Center, Cincinati, Ohio.

DISTRIBUTION

COMMANDER IN CHIEF
U.S. ATLANTIC FLEET
ATTN: NSAP SCIENCE ADVISOR
NORFOLK, VA 23511

CINCUSNAVEUR
ATTN: NSAP SCIENCE ADVISOR
BOX 100
FPO NEW YORK 09510

COMSECONDFLT
ATTN: NSAP SCIENCE ADVISOR
FPO NEW YORK 09501-6000

COMTHIRDFLT
ATTN: NSAP SCIENCE ADVISOR
PEARL HARBOR, HI 96860-7500

COMSEVENTHFLT
ATTN: NSAP SCIENCE ADVISOR
BOX 167
FPO SEATTLE 98762

COMSIXTHFLT/COMFAIRMED
ATTN: NSAP SCIENCE ADVISOR
FPO NEW YORK 09501-6002

COMMANDER NAVAL AIR FORCE
U.S. ATLANTIC FLEET
ATTN: NSAP SCIENCE ADVISOR
NORFOLK, VA 23511-5188

COMNAVAIRPAC
ATTN: NSAP SCIENCE ADVISOR
NAS, NORTH ISLAND
SAN DIEGO, CA 92135

COMNAVSURFLANT
ATTN: NSAP SCIENCE ADVISOR
NORFOLK, VA 23511

COMNAVSURFPAC
(005/N6N)
ATTN: NSAP SCIENCE ADVISOR
SAN DIEGO, CA 92155-5035

COMMANDER
MINE WARFARE COMMAND
ATTN: NSAP SCIENCE ADVISOR
CODE 007
CHARLESTON, SC 29408-5500

COMMANDER
OPTEVFOR
ATTN: NSAP SCIENCE ADVISOR
NORFOLK, VA 23511-6388

COMMANDER
SURFACE WARFARE DEV. GROUP
NAVAMPHIB BASE, LITTLE CREEK
NORFOLK, VA 23521

COMFLTAIR, MEDITERRANEAN
ATTN: NSAP SCIENCE ADVISOR
CODE 03A
FPO NEW YORK 09521

COMMANDING GENERAL
MARINE AMPHIBIOUS FORCE FMF
ATTN: NSAP SCI. ADV.
CAMP PENDLETON, CA 92055

COMMANDING GENERAL (G4)
FLEET MARINE FORCE, ATLANTIC
ATTN: NSAP SCIENCE ADVISOR
NORFOLK, VA 23511

USCINCENT
ATTN: WEATHER DIV. (CCJ3-W)
MACDILL AFB, FL 33608-7001

ASST. FOR ENV. SCIENCES
ASST. SEC. OF THE NAVY (R&D)
ROOM 5E731, THE PENTAGON
WASHINGTON, DC 20350

CHIEF OF NAVAL RESEARCH (2)
LIBRARY SERVICES, CODE 784
BALLSTON TOWER #1
800 QUINCY ST.
ARLINGTON, VA 22217-5000

CHIEF OF NAVAL OPERATIONS
(OP-006)
U.S. NAVAL OBSERVATORY
WASHINGTON, DC 20390

CHIEF OF NAVAL OPERATIONS
OP-953
NAVY DEPARTMENT
WASHINGTON, DC 20350

OFFICE OF NAVAL TECHNOLOGY
MAT-0724, NAVY DEPT.
800 N. QUINCY ST.
ARLINGTON, VA 22217

COMMANDANT OF THE MARINE CORPS
HDQ, U.S. MARINE CORPS
WASHINGTON, DC 20380

DIRECTOR
NATIONAL SECURITY AGENCY
ATTN: LIBRARY (2C029)
FT. MEADE, MD 20755

DIRECTOR
DEFENSE NUCLEAR AGENCY
WASHINGTON, DC 20305

CHIEF, ENV. SVCS. DIV.
OJCS (J-33)
RM. 2877K, THE PENTAGON
WASHINGTON, DC 20301

NAVAL DEPUTY TO THE
ADMINISTRATOR, NOAA
ROOM 200, PAGE BLDG. #1
3300 WHITEHAVEN ST. NW
WASHINGTON, DC 20235

COMMANDING OFFICER
NAVAL RESEARCH LAB
ATTN: LIBRARY, CODE 2620
WASHINGTON, DC 20390

COMMANDING OFFICER
OFFICE OF NAVAL RESEARCH
1030 E. GREEN ST.
PASADENA, CA 91101

OFFICE OF NAVAL RESEARCH
SCRIPPS INSTITUTION OF
OCEANOGRAPHY
LA JOLLA, CA 92037

COMMANDING OFFICER
NAVAL OCEAN RSCH & DEV ACT
NSTL, MS 39529-5004

COMMANDER
OCEANOGRAPHIC SYSTEMS PACIFIC
BOX 1390
PEARL HARBOR, HI 96860

COMMANDER
NAVAL OCEANOGRAPHY COMMAND
NSTL, MS 39529-5000

COMMANDING OFFICER
NAVAL OCEANOGRAPHIC OFFICE
BAY ST. LOUIS
NSTL, MS 39522-5001

COMMANDING OFFICER
FLENUMOCEANCEN
MONTEREY, CA 93943-5005

SUPERINTENDENT
LIBRARY REPORTS
U.S. NAVAL ACADEMY
ANNAPOLIS, MD 21402

CHAIRMAN
OCEANOGRAPHY DEPT.
U.S. NAVAL ACADEMY
ANNAPOLIS, MD 21402

DIRECTOR OF RESEARCH
U.S. NAVAL ACADEMY
ANNAPOLIS, MD 21402

SUPERINTENDENT
NAVPGSCOL
MONTEREY, CA 93943-5000

NAVAL POSTGRADUATE SCHOOL
METEOROLOGY DEPT.
MONTEREY, CA 93943-5000

NAVAL POSTGRADUATE SCHOOL
OCEANOGRAPHY DEPT.
MONTEREY, CA 93943-5000

NAVAL POSTGRADUATE SCHOOL (25)
PHYSICS & CHEMISTRY DEPT.
MONTEREY, CA 93943-5000

LIBRARY
NAVAL POSTGRADUATE SCHOOL
MONTEREY, CA 93943-5002

PRESIDENT
NAVAL WAR COLLEGE
GEOPHYS. OFFICER, NAVOPS DEPT.
NEWPORT, RI 02841

COMMANDER (2)
NAVAIRSYSCOM
ATTN: LIBRARY (AIR-723D)
WASHINGTON, DC 20361-0001

COMMANDER
NAVAIRSYSCOM (AIR-330)
WASHINGTON, DC 20361-0001

COMMANDER
NAVAIRSYSCOM
MET. SYS. DIV. (AIR-553)
WASHINGTON, DC 20360

COMMANDER, SPACE & NAVAL
WARFARE SYSTEMS COMMAND
ATTN: CAPT. K. VAN SICKLE
CODE 06G, NAVY DEPT.
WASHINGTON, DC 20363-5100

COMMANDER
NAVAL SEA SYSTEMS COMMAND
ATTN: LT S. PAINTER
PMS-405-24
WASHINGTON, DC 20362-5101

COMMANDER
NAVOCEANSYSCEN
DR. J. RICHTER, CODE 54
SAN DIEGO, CA 92152-5000

COMMANDER
NAVAL WEAPONS CENTER
DR. A. SHLANTA, CODE 3331
CHINA LAKE, CA 93555-6001

COMMANDER
NAVAL SHIP RSCH & DEV. CENTER
CODE 5220
BETHESDA, MD 20084

COMMANDER
NAVSURFWEACEN, CODE R42
DR. B. KATZ, WHITE OAKS LAB
SILVER SPRING, MD 20910

DIRECTOR
NAVSURFWEACEN, WHITE OAKS
NAVY SCIENCE ASSIST. PROGRAM
SILVER SPRING, MD 20910

COMMANDER
NAVAL SURFACE WEAPONS CENTER
ATTN: CODE 44
DAHLGREN, VA 22448-5000

COMMANDING OFFICER
AMPHIBIOUS WARFARE LIBRARY
NAVAL AMPHIBIOUS SCHOOL
NORFOLK, VA 23521

COMMANDER
AWS/DN
SCOTT AFB, IL 62225

USAFETAC/TS
SCOTT AFB, IL 62225

COMMANDER
ARMY DEFENSE & READINESS COM
ATTN: DRCLDC
5001 EISENHOWER AVE.
ALEXANDRIA, VA 22304

DEPT. OF THE ARMY
CHIEF OF ENGINEERS OFFICE
ATTN: DAEN-RDM
WASHINGTON, DC 20314

COMMANDER & DIRECTOR
ATTN: DELAS-D
U.S. ARMY ATMOS. SCI. LAB
WHITE SAND MISSILE RANGE
WHITE SANDS, NM 88002

COMMANDING OFFICER
U.S. ARMY RESEARCH OFFICE
ATTN: GEOPHYSICS DIV.
P.O. BOX 12211
RESEARCH TRIANGLE PARK, NC
27709

DIRECTOR
LIBRARY, TECH. INFO. CEN.
ARMY ENG. WATERWAYS STN.
VICKSBURG, MS 39180

COMMANDER & DIRECTOR
ATTN: DELAS-AS
U.S. ARMY ATMOS. SCI. LAB
WHITE SANDS MISSILE RANGE,
NEW MEXICO 88002

COMMANDER & DIRECTOR
U.S. ARMY ATMOS. SCI. LAB.
ATTN: DELAS-AF
WSMR, NEW MEXICO 88002

COMMANDER/DIRECTOR
US ARMY ATMOS. SCIENCE LAB.
ATTN: DELAS-AT-0
WHITE SANDS MISSILE RANGE, NM
88002

DIRECTOR (12)
DEFENSE TECH. INFORMATION
CENTER, CAMERON STATION
ALEXANDRIA, VA 22314

DIRECTOR, TECH. INFORMATION
DEFENSE ADV. RSCH PROJECTS
1400 WILSON BLVD.
ARLINGTON, VA 22209

COMMANDANT
U.S. COAST GUARD
WASHINGTON, DC 20226

HEAD, ATMOS. SCIENCES DIV.
NATIONAL SCIENCE FOUNDATION
1800 G STREET, NW
WASHINGTON, DC 20550

DIRECTOR
FEDERAL EMERGENCY MANAGEMENT
AGENCY (FEMA)
WASHINGTON, DC 20472

DR. MARVIN DICKERSON
L-262, LLNL
P.O BOX 808
LIVERMORE, CA 94550

ROGER HELVEY, CODE 3253 (4)
PACMISTESTCEN
PT. MUGU, CA 93042

STUART GATHMAN, CODE 4117
NAVAL RESEARCH LAB
WASHINGTON, DC 20375

JIM BRANUM
2682 OLIVESTONE WAY
SAN JOSE, CA 95132

END
DTIC
8-86